Hans Chr. Sørensen

SHEAR TESTS ON 12 REINFORCED CONCRETE T-BEAMS

RAPPORT NR. R 60 1974

PREFACE

This report, together with the report Sørensen [70.1] has been prepared as a part of the work required for the Ph.D-degree in civil engineering ("lic.techn.degree").

The principal assignment in the Ph.D-studies has been to

> "give a review and an evaluation of theory and tests on shear strength of reinforced concrete beams, possibly supplemented by own tests."

The studies have been carried out at the Structural Research Laboratory of the Technical University of Denmark, under Professor, dr.techn. K.W.Johansen. Dr.techn. H.Krenchel has acted as adviser on the work.

In addition, I have received valuable assistance in the execution of the tests from many colleagues at the Laboratory.

I should like to thank Professor, dr.techn. T.C.Hansen of the Laboratory for Building Materials for giving me the opportunity of using the tests in series II as 4th year exercises for civil engineering students. I also wish to express my gratitude to the students for their assistance in the execution of the tests. Finally, I should like to mention Danmarks Ingeniørakademi's Building Division, who kindly lent me their datalogger equipment in connexion with the tests in series I.

Copenhagen, December 4, 1970

Hans Chr.Sørensen *

This report is a translation of the Danish report Sørensen [71.1]. I should like to thank Mrs. P.Katborg for the translation.
Lyngby, August 2nd, 1974

Hans Chr.Sørensen

---

* Now: Head of department of concrete technology
Aalborg Portland R & D, Concrete Research Laboratory,
Karlstrup, 2690 Karlslunde, Denmark.

CONTENTS

SUMMARY

This report describes tests on 12 reinforced concrete T-beams subjected to combined bending and shear. The tests are a continuation of earlier tests carried out in 1963-1965 by K.Özden [67.1].

All the beams had a shear span $\frac{M}{Vd} = 3.5$, a longitudinal ratio $\rho_o = 1.06\%$, and a concrete cylinder strength $f_c = 250\text{-}330$ kp/cm^2 (fig.1.1, 2.3 and 2.4 and table I). Only the shear reinforcement (vertical stirrups of mild plain bars) was varied (table I and fig.1.2).

Strain measurements by means of 100-130 strain-gauges were taken on 3 of the beams (series I: T21, T22 and T23). The strain -gauge measurements on the concrete compression flange (fig.1.3 and table IIa-c) and the crack formation (fig.2.9) indicate the precense of an arch action in the shear span. The strain-gauge measurements on the longitudinal reinforcement (fig.1.5 and table IIIa-c) indicate a considerable dowel action even at 60% of the ultimate load. The strain-gauge measurements on the stirrups (fig.1.7 and table IVa-c) and the measurements of the maximum crack widths indicate the possibility of utilizing stirrups with a yield strength (0.2% off-set) of about 6000 kp/cm^2.

The ultimate load (table I and fig.1.2), compared with two typical shear formulae, shows that Hillerborg's formulae [68.1] are in good agreement with the test results, whereas those of ACI [62.1] underestimate the shear failure load by about 60%.

Most of the notation in this report is in accordance with that of CEB [73.1].

NOTATION

Most of notation is in accordance with that used by CEB [73.1]. The following indices and symbols are used throughout:

Indices:

c	Concrete
s	Longitudinal reinforcement
u	Ultimate load
v	Web reinforcement
y	Yield strength (~0.2% off-set)
A(B)	Corresponding internal force referred to normal cross-section A-A(B-B)
F	Failure load in flexure

Symbol

A	Cross-sectional area of reinforcement
E	Young's modulus of elasticity
M	Flexural moment
N_a	Tensile normal force in longitudinal reinforcement
V	Shear force
V_s, V_b	Part of shear force resisted by longitudinal reinforcement (dowel action) and concrete compression zone, respectively
$\emptyset_v$	Diameter of single stirrup-leg
a	Shear span
b	Width of compression flange
b_w	Width of web
c	Length of projection of diagonal crack on axis of the beam
d	Effective depth of longitudinal reinforcement
f	Strength
f_c	Cylinder compressive strength of concrete
f_{sp}	Splitting tensile strength of concrete (Brazilian test)
n	Number of stirrups in shear span
s	Distance between stirrups measured parallel to axis of the beam
z	Lever arm
δ	Coefficient of variation
ε	Strain, positive as tension, negative as compression
ρ_o	Ratio of longitudinal reinforcement A_s/bd
ρ_{so}	Ratio of longitudinal reinforcement $A_s/b_w d$
θ	Idealized angle between diagonal crack and axis of beam
σ	Stress

1. SUMMARY OF TESTS

1.1 Introduction

At the Structural Research Laboratory of the Technical University of Denmark, in the period from 1963 to 1965, 16 shear tests were carried out on T-beams, in which the only variable was the web reinforcement - Özden [67.1]. *

In half the beams, the web reinforcement consisted of relatively widely spaced vertical stirrups. The tests show that just a single stirrup placed where the diagonal crack forms will result in a considerable increase in the ultimate strength of the beam compared with that of beams without web reinforcement. Corresponding results have been achieved by Kani [69.1] and others. In the remaining tests, the web reinforcement consisted of bent -up longitudinal reinforcement, and the paper Sørensen [74.1] deals with these tests.

This report includes the results of a further 12 shear tests on T-beams in which the web reinforcement consisted of relatively closely spaced stirrups. These tests were carried out in 1969, as a supplement to Özden's tests. Sections 1.2 to 1.5 contain a short description of these tests, while Section 2 provides a thorough analysis of the test conditions, together with a number of tables giving the test results.

1.2 Test programme

All the beams testet were T-beams, simply supported and loaded with two symmetrical, point loads acting perpendicular to the axis of the beam ($\frac{M}{Vd} = 3.5$), see also Fig.1.1 and section 2.2. The longitudinal reinforcement consisted of deformed bars (Kamstål) with a nominal diameter of 20 mm and a yield strength f_{sy} of about 4300 kp/cm^2 - a total of 4 K 20 in two layers (ratio of reinforcement $\rho_o = 1.06\%$, $\rho_{so} = 3.84\%$, see also Section 2.1.3).

---

* References are listed in Section 1.5

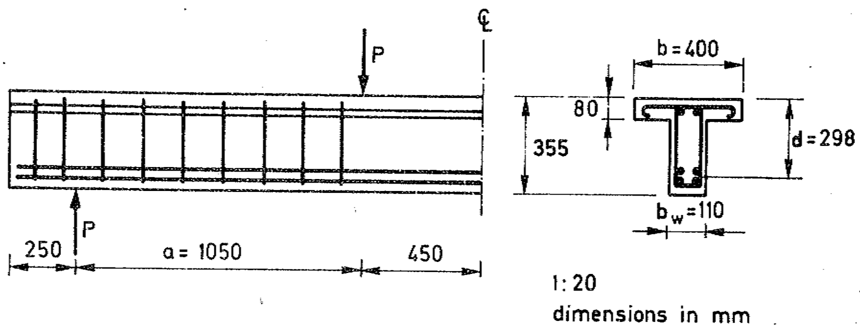

Fig.1.1: Experimental beam

A cylinder compressive strength of $f_c = 325$ kp/cm² was aimed at for the concrete, together with a water/cement-ratio of $w/c = 0.71$. However, the quality of the cement varied considerably, so that the target cylinder strength was only achieved in three of the beams (series I), while in the remainder (series II) it was about 250 kp/cm². Table I (Section 1.3.1) shows the values of f_c for the various beams, and Sections 2.1.1 and 2.1.2 give the composition of the concrete and the results achieved in the stress-strain measurements.

The web reinforcement consisted of vertical stirrups of plain, mild steel with a yield strength of $f_{vy} = 2300\text{-}4500$ kp/cm². The variation in the web reinforcement consisted partly of an alteration of the stirrup spacing s and partly of an alteration in the nominal diameter $\emptyset_v$ of the stirrups (and thereby also of their yield strength f_{vy}). Table I in Section 1.3.1 shows the value of $\emptyset_v$, s and $A_v f_{vy} \frac{d}{s}$, where A_v is the nominal area of the stirrups, and d is the effective depth. The quantity $A_v \cdot f_{vy} \cdot \frac{d}{s}$ denotes the total yield force in the area of diagonal cracking, corresponding to an angle between the diagonal crack and the axis of the beam $\theta = 45^\circ$.

Section 2.1.6 shows the stress-strain diagrams for the reinforcing bars, the geometry of the stirrups and their placing.

For beams T21 and T22, table I shows two values of $A_v f_{vy} \frac{d}{s}$, due to the fact that the yield strength f_{vy} for the stirrups in question is only known to lie between two values corresponding to an investigation of f_{vy} before the test and one after the test. See, further, Section 2.1.6.

The tests are classified in two groups, Series I and Series II, according to the measurements taken during the tests.

In series I, the strain in the longitudinal reinforcement, along the surface of the compression flange and on the stirrups was measured by means of 100-130 strain-gauges on each beam. In addition, the deflection at the top and bottom of the beam was measured at a total of 13-17 points. The total deformations were measured along the longitudinal reinforcement (5 lengths) and along the compression flange in the bending span. Finally, the crack pattern was registered, and the maximum widths of cracks were measured.

In series II, which consisted of nine beams, the total deformations along the longitudinal reinforcement and the compression flange in the bending span were measured, and the crack was registered.

The locations of the measuring points are shown in Fig.2.3 and 2.4 of Section 2.

1.3 Results

1.3.1 Ultimate load

Table I shows the ultimate load and type of failure for the various beams, including specification of the end of the beam at which failure occurred (for the orientation of the beams, reference is made to Fig.2.7 in Section 2.2.1). Table I also gives the length of the horizontal projection c of the diagram crack (see Fig.1.5) in relation to the effective depth d. The magnitude of c appeared from the cracked beam, in that a flexural tensile crack was clearly apparent from the point of intersection of the biggest diagonal crack with the longitudinal reinforcement to the bottom of the beam, approximately perpendicular

Table I: Shear reinforcement, concrete strength, ultimate load and type of failure

	Beam no	$Ø_v$ mm	s mm	$A_v f_{vy} \frac{d}{s}$ Mp	P_u [1)] Mp	f_c kp/cm²	Type of [2)] failure		$\frac{c}{d}$
Serie I	T21	R8	175	3.96-4.67	13.2	331	DT	-	2.2
	T22	R7	210	4.43-4.95	13.0	317	DT/SC	-	1.6
	T23	R6	150	3.98	14.2	349	DT	+	2.5
Serie II	T1a	R6	87.5	5.09	13.5	234	F		
	T2a	R5	87.5	5.42	13.9	251	F		
	T3a	R6	105	4.24	13.0	251	AS	-	1.9
	T4a	R5	105	4.52	13.5	257	AS	-	1.9
	T1b	R6	117	3.80	12.0	236	AS-SC	+	1.6
	T2b	R5	117	4.05	13.2	254	DT	-	1.8
	T3b	R6	175	2.54	11.8	251	AS-DT	-	2.3
	T4b	R5	175	2.71	10.9	252	DT	+	2.0
	T5	R5	175	2.71	11.2	260	AS-DT	-	2.0

1) Exclusive of weight of beam 0.15 Mp/m

2) F Flexure failure
SC Shear compression failure
DT Diagonal tension failure
AS Arch stability failure

\+ or - mention in what end of the beam the failure took place (Fig.2.7, chapter 2.2.1.

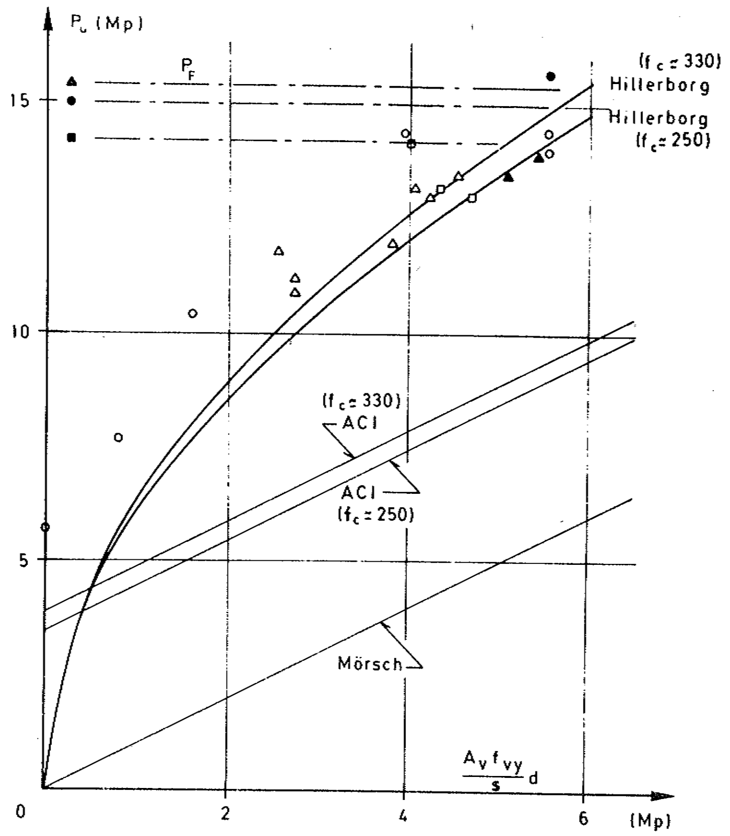

○ □ $f_c \simeq$ 330 kp/cm²
△ $f_c \simeq$ 250 kp/cm²
○ Özden [67.1]
□ Series I
△ Series II
□△○ Shear failure
▲● Flexural failure

Fig.1.2: Ultimate load as function of the intensity of web reinforcement for beams in series I and II and for some of Özden's beams [67.1]

to the axis of the beam (see also Fig.2.9).

In Fig.1.2 the ultimate load is depicted as a function of $A_v f_{vy} \frac{d}{s}$ (corresponding to the contribution of the stirrups to the shear strength at an angle of $\theta = 45^o$ between the diagonal crack and the beam axis). The figure also shows the results of eight of Özden's tests [67.1]. As, in some of Özden's tests, only one or two stirrups were located in the shear span, whereby the stirrup spacing could not be defined, s in these cases has been calculated by distributing the stirrup force over the entire length a of the shear span, i.e.

$$A_v \ f_{vy} \frac{d}{s} = A_v \ f_{vy} \frac{d}{a} n \qquad (1.1)$$

where n is the number of stirrups in the shear span (n = 1 or 2).

In the case of beams T21 and T22 from series I, the average value of the limits given in table I is used for $A_v \ f_{vy} \frac{d}{s}$ in Fig.1.2.

Fig.1.2 shows the expected flexural failure load P_F calculated from the expression

$$P_F = \frac{M_F}{a} = A_s \ f_{sy} \frac{z}{a} = \frac{d}{a} A_s \ f_{sy} (1-0.5 \ \rho_o \frac{f_{sy}}{f_c}) \qquad (1.2)$$

where z is the lever arm.

The figure also shows the expected shear failure load P_u, calculated in accordance with Hillerborg (see, e.g. Sørensen [70.1] or Regan [68.1]:

$$P_u = 9.5 (f_c)^{1/6} (\rho_{so})^{1/4} (A_v \ f_{vy} \frac{d}{s})^{1/2} (b_w d)^{1/2} \qquad (1.3)$$

where the unit system is kp, cm. Furthermore, P_u is calculated in accordance with ACI [62.1] (Modified Thruss Analogy):

$$P_u = P_{cr} + A_v \ f_{vy} \frac{d}{s} \leq 2.65 \sqrt{f_c} \ b_w d \qquad (1.4)$$

where the diagonal crack load P_{cr} is calculated from

$$P_{cr} = (0.50\sqrt{f_c} + 176\frac{\rho_{so}}{\frac{a}{d}-1})b_w d \leq 0.93\sqrt{f_c}\,b_w d \quad (1.5)$$

Unit system kp, cm.

Finally, the expected shear ultimate load P_u according to Mörsch (Thruss Analogy) is also given:

$$P_u = A_v f_{vy}\frac{d}{s} \quad (1.6)$$

As will be seen from Fig.1.2, Hillerborg's formulae gives satisfactory accordance with the test results, while the other formulae yield very conservative values.

1.3.2 Strain measurements along the concrete compression flange (series I)

Fig.1.3 shows the development of strain at a few loading stages along the middle of the surface of the concrete compression flange of beam T23. It will be seen that there are considerable tensile stresses in the concrete at the supports. Near failure,

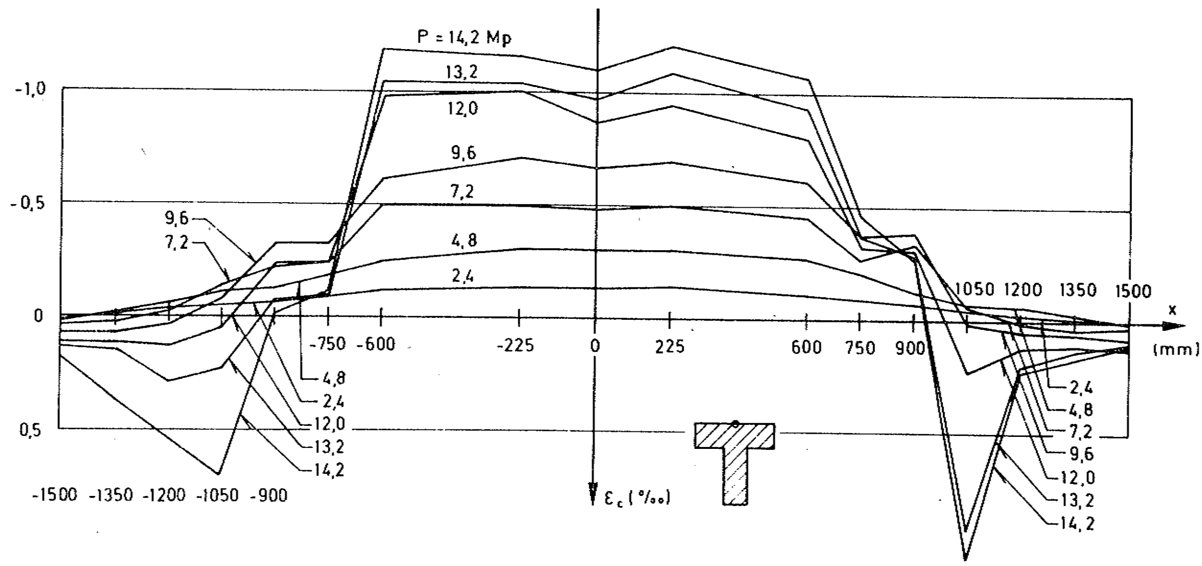

Fig.1.3: Development of strain along middle of surface of compression flange in beam T23 (Table IIc)

these tensile stresses increase rapidly, indicating a considerable arch action. This arch action is also apparent from the cracks in the top of the flange in the crack pattern shown in Fig.2.9 (Section 2.4). Corresponding conditions apply in the case of the other two beams in series I.

Table IIa-c (Section 2.4) shows the strains for the three beams in series I.

1.3.3 Strain and force in longitudinal reinforcement (series I)

Fig.1.4 shows the force N_s in the longitudinal reinforcement of beam T23 at a number of loading stages, calculated on the basis of strain-gauge measurements as given in table IIIc (Section 2.4).

For the diagonally cracked beam in Fig.1.5, it is found from the equilibrium equations that N_s in cross-section A-A can be determined from the expression

$$N_s = \frac{M_A}{z} + V_c \frac{c}{z} + \frac{1}{2} A_v f_{vy} \frac{c^2}{sz} \qquad (1.7)$$

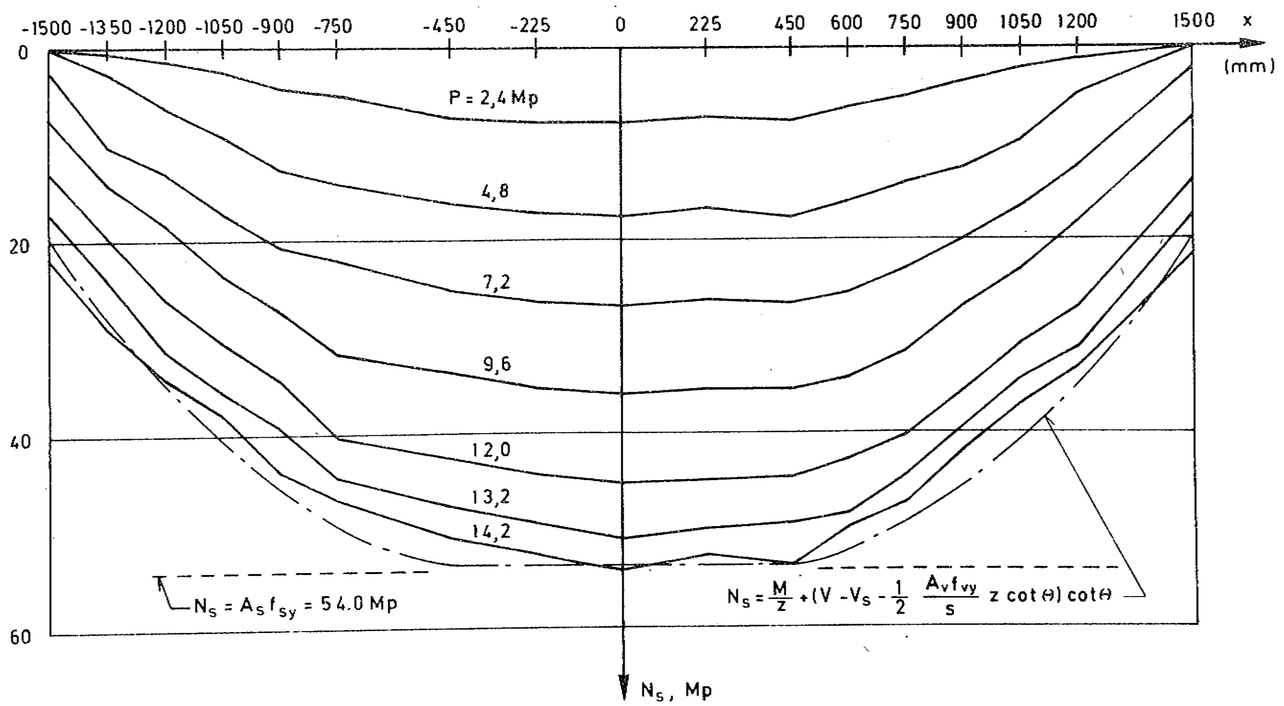

Fig.1.4: Tensile force in the longitudinal reinforcement of beam T23 (Table IIIc)

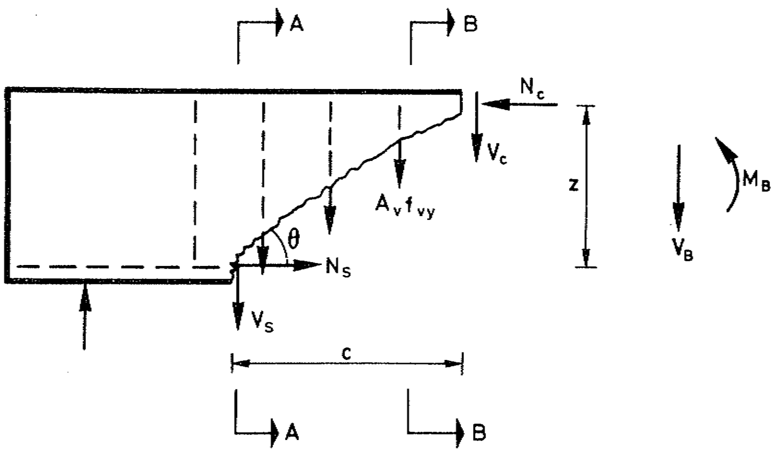

Fig.1.5: Internal forces in diagonally cracked beam

where M_A is the bending moment in cross-section A-A, and V_c is the contribution of the concrete compression flange to the shear strength. Denoting the contribution of the longitudinal reinforcement (dowel action) to the shear strength V_s, we get for the total shear force V:

$$V = V_s + V_c + A_v f_{vy} \frac{c}{s} \tag{1.8}$$

Introducing the average inclination of the diagonal crack θ,

$$\cot \theta = \frac{c}{z} \tag{1.9}$$

and inserting V_c from (1.8) in (1.7), we get

$$N_s = \frac{M_A}{z} + (V - V_s - 1/2\, A_v f_{vy} \frac{z}{s} \cot \theta) \cot \theta \tag{1.10}$$

The value of N_s calculated in accordance with this expression is shown in Fig.1.4, where V is set equal to the ultimate value P_u, the lever arm z is calculated corresponding to pure bending (last term in equation (1.2), and $\cot\theta$ is put equal to zero in the bending span and is calculated proportional to the distance of the section in question from the loading cross-section ($x = \pm 450$ mm), whereby $\cot\theta = \frac{a}{z}$ at the support. The dowel action is taken into account by introducing a contribution corresponding to the yield force $A_v\ f_{vy}$ of a single stirrup. Then, at the distance $c = z \cot\theta$ from the cross-section under load, we get

$$N_s = P_u\ \frac{a}{z} - A_v\ f_{vy}(1 + \frac{1}{2}\ \frac{z}{s}\ \cot\theta)\cot\theta \qquad (1.11)$$

It will be seen from Fig.1.4 that this expression gives a result that is in reasonable agreement with the strain-gauge measurements.

To investigate the dowel action, Fig.1.6a-c shows the strain in the top and bottom of the longitudinal reinforcement for three characteristic cross-sections - also in beam T23.

The development of strain in the cross-section in pure flexure (fig.1.6a) shows that the strain at all measuring points was very near yielding (ε_{sy}), which indicates that the load was close to the flexural failure load, as can also be seen from Fig. 1.2.

The development of strain shown in Fig.1.6b, is from a section located directly in front of the intersection of the biggest diagonal crack with the longitudinal reinforcement (cf. crack pattern shown in Fig.1.10). It will be seen from this there is heavy local curvature in the various reinforcing bars and that the two layers of reinforcement have slipped in relation to each other. This witnesses to a certain degree of dowel action, which is already prominent at about 60% of the ultimate load.

The development of strain in the cross-section at the support (Fig.1.6c) shows clearly that there is a definite dowel action in the longitudinal reinforcement, since not only the individual reinforcing bars, but also the two layers of reinforcement together, show the opposite curvature to that in the section shown in Fig.1.6b.

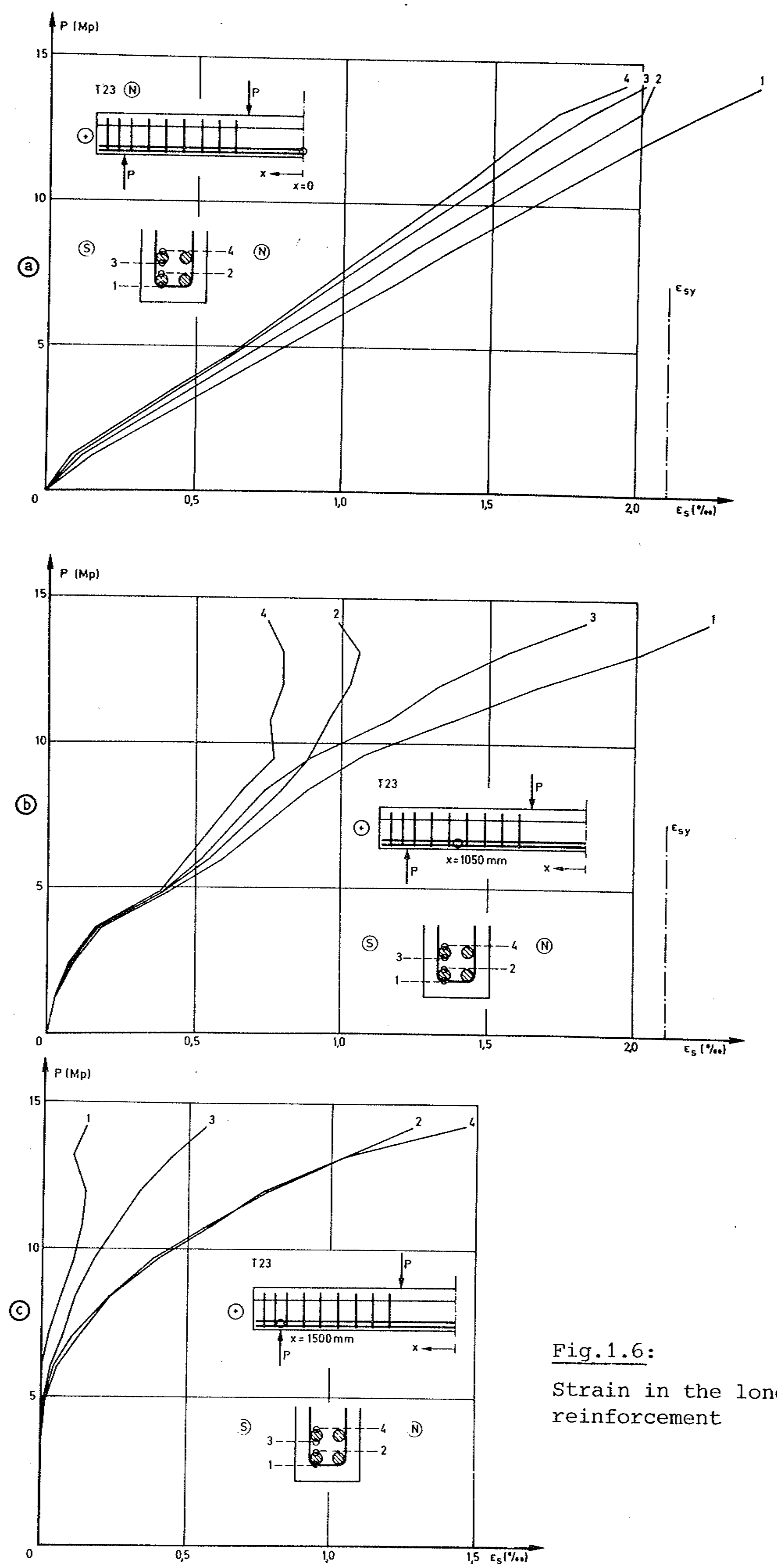

Fig.1.6:

Strain in the longitudinal reinforcement

1.3.4 Strain in stirrups (series I)

Fig.1.7 shows the strain in four of the stirrups in beam T23 as a function of the load. It will be seen from this and from table IV (Section 2.4) that the strain reached yielding in all stirrups except those in the immediate proximity of the loading cross-section and the support. Corresponding conditions have been found by, inter alios, Leonhardt and Walther [63.1].

Even at about 85% of the ultimate load, the strain already exceeds 0.4% in several of the stirrups, which - compared with the crack measurements (table VIII) - indicates that it should be possible to utilize stirrups with a much higher yield strength, e.g. stirrups of Tentor steel (Danish cold worked, deformed bars with $f_{vy} = 5600$ kp/cm^2).

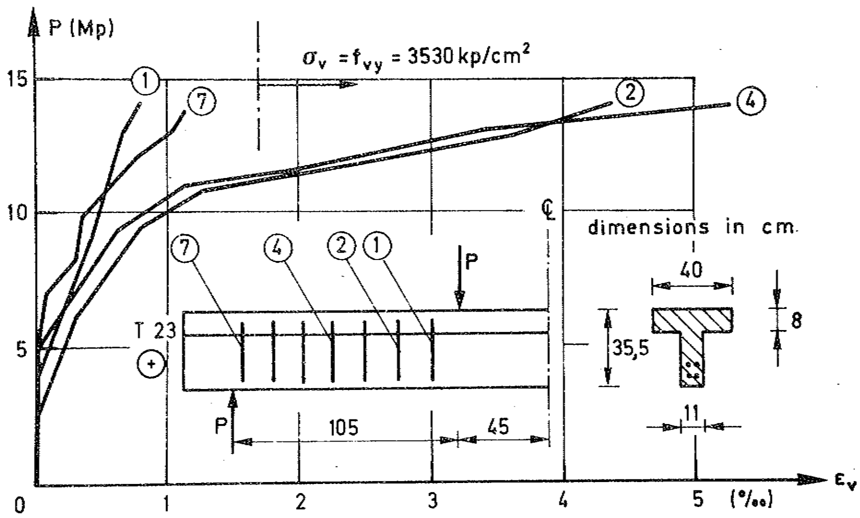

Fig.1.7: Development of strain in some of the stirrups of beam T23 (Table IVc)

1.3.5 Deflection measurements (series I)

Fig.1.8 shows the deflections on the tensile and compression flanges of beam T23. As the basis for measuring these deflections, use has been made in both cases of the line connecting two points at a distance of ±1575 mm from the centre of the beam.

As will be seen from the figure, there is a considerable difference in the two lines of deflection in the shear span when the load exceeds about 50% of the ultimate load. This is due to the opening of the diagonal cracks.

1.3.6 Measurements with dial gauges

Fig.1.9 shows the mean strain along the bottom layer of longitudinal reinforcement in beam T23 in series I, measured with dial gauges outside the concrete (table VIc, Section 2.4). For the

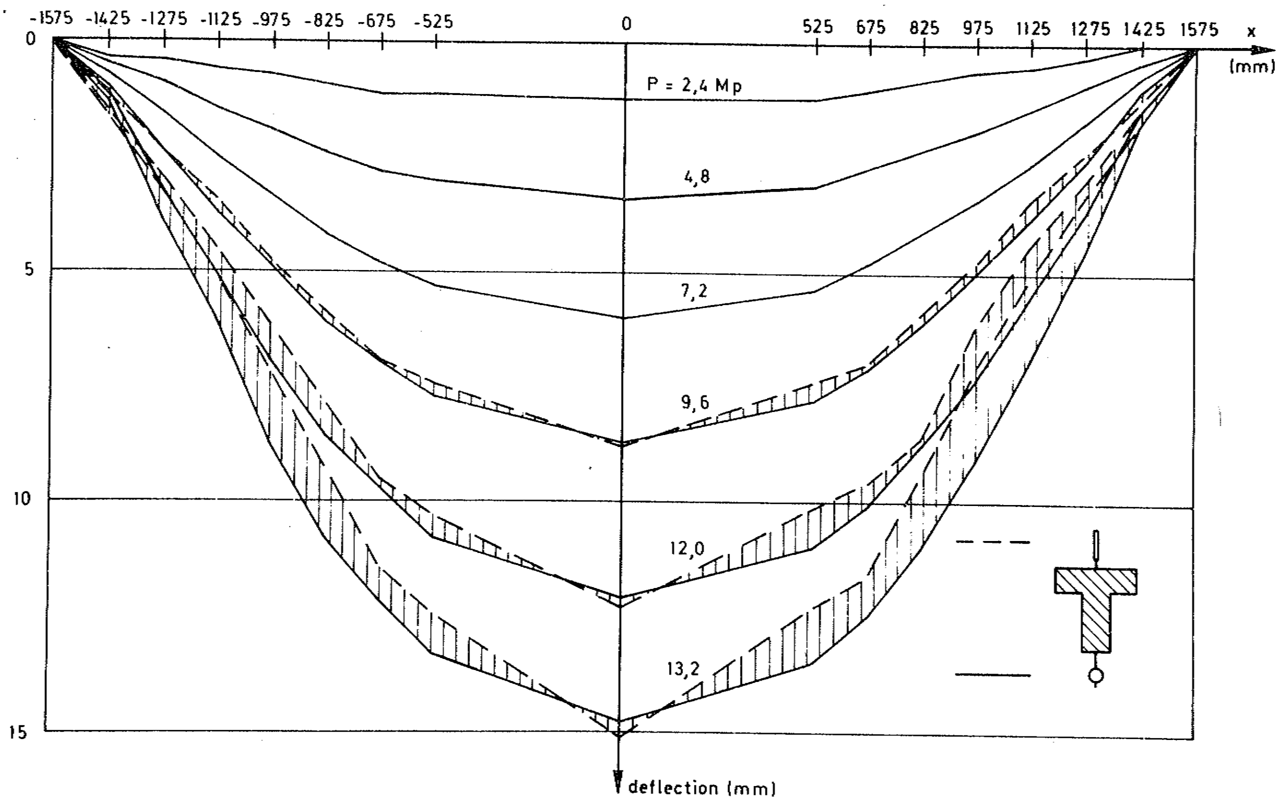

Fig.1.8: Deflection of tensile and compression flanges (Table Vc)

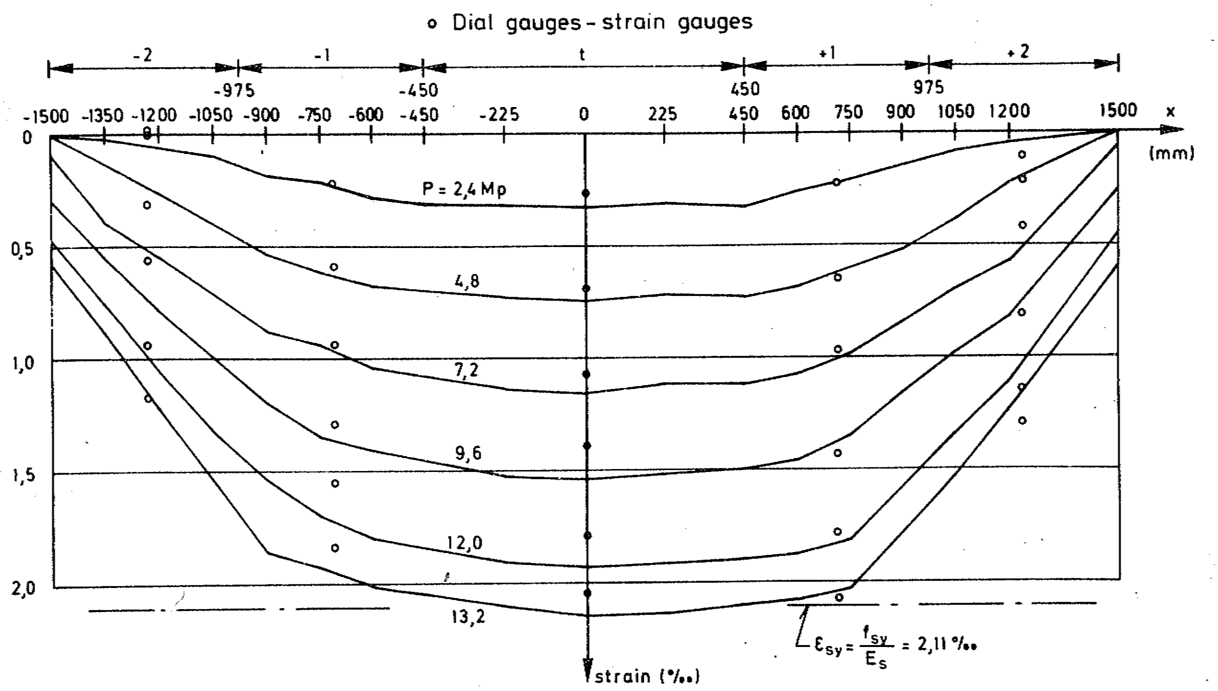

Fig.1.9: Comparison of strain measurements with strain-gauges and with dial gauges on beam T23 (Table IIIc and VIc)

purposes of comparison, the corresponding strain values measured by means of strain-gauges are also shown. It will be seen that the dial gauge measurements deviate about 10% from the strain -gauge measurements. In the bending span, the dial gauge measurements always give too low values, and this is the case in the shear span too, up to about 60% of the ultimate load. Closer to failure, the dial gauge measurements do not give a correct picture of the strain in the individual layers of reinforcement. Thus strain measurements on the concrete cannot be expected to reflect the dowel action discussed in Section 1.3.3.

1.3.7 Crack formation and crack widths

Fig.1.10 shows the crack development in beam T23 of series I. It will be seen that the first diagonal crack forms as a bending shear crack at an angle of about 45^{o} with the axis of the beam. As the load is gradually increased, several corresponding diagonal cracks form in the shear span at a distance of about the stirrup spacing. The maximum widths of the diagonal cracks are comparatively modest (less than 0.3 mm) up to about 75% of the ultimate load, as will be seen from table VIII in Section 2.4. This indicates that the strain in the stirrups is still in the elastic range, cf. Fig.1.7. When the load is now increased, the width of the cracks increases considerably, and no more diagonal cracks form at 45° with the axis of the beam. There is a tendency for flatter diagonal cracks to occur between those already formed as the load is increased. Prior to the failure, the diagonal cracks extend up to the compression flange, and tensile cracks form at the top of this flange, indicating a certain arch action. The beam fails when the compression flange is traversed by a single crack and two diagonal cracks are joined up by horizontal crack along the longitudinal reinforcement, which then breaks out (failure of dowel action).

Table VIII in Section 2.4 gives the maximum crack widths for the beams in series I at a number of loading stages.

The crack patterns at failure for all beams are shown in Fig. 2.9a-n in Section 2.4. The development of the cracking will also be seen by the numbering of the cracks, as described in Section 2.3.7.

A comparison of the crack patterns on the two sides of the beams (N and S) shows that these were largely symmetrical, despite the fact that, in series I, twice as many strain-gauge wires were led out through the S-side of the beams as through the N-side.

A comparison of the crack patterns for the beams in series I and series II shows no significant difference. This accords with the fact that the diagonal cracks observed in the beams in series I did not tend particulary to originate from points at which the wires were led out of the web of the beam.

It will be seen from table I (Section 1.3.1) that about 2/3 of the beams ruptured at the end of the shear span designated by a minus (-) (se definition Fig.2.7, Section 2.2.1), possibly due to the loading arrangement shown there. However, the crack development and strain measurements showed definite symmetry in the two shear spans, and it was not possible until immediately be-

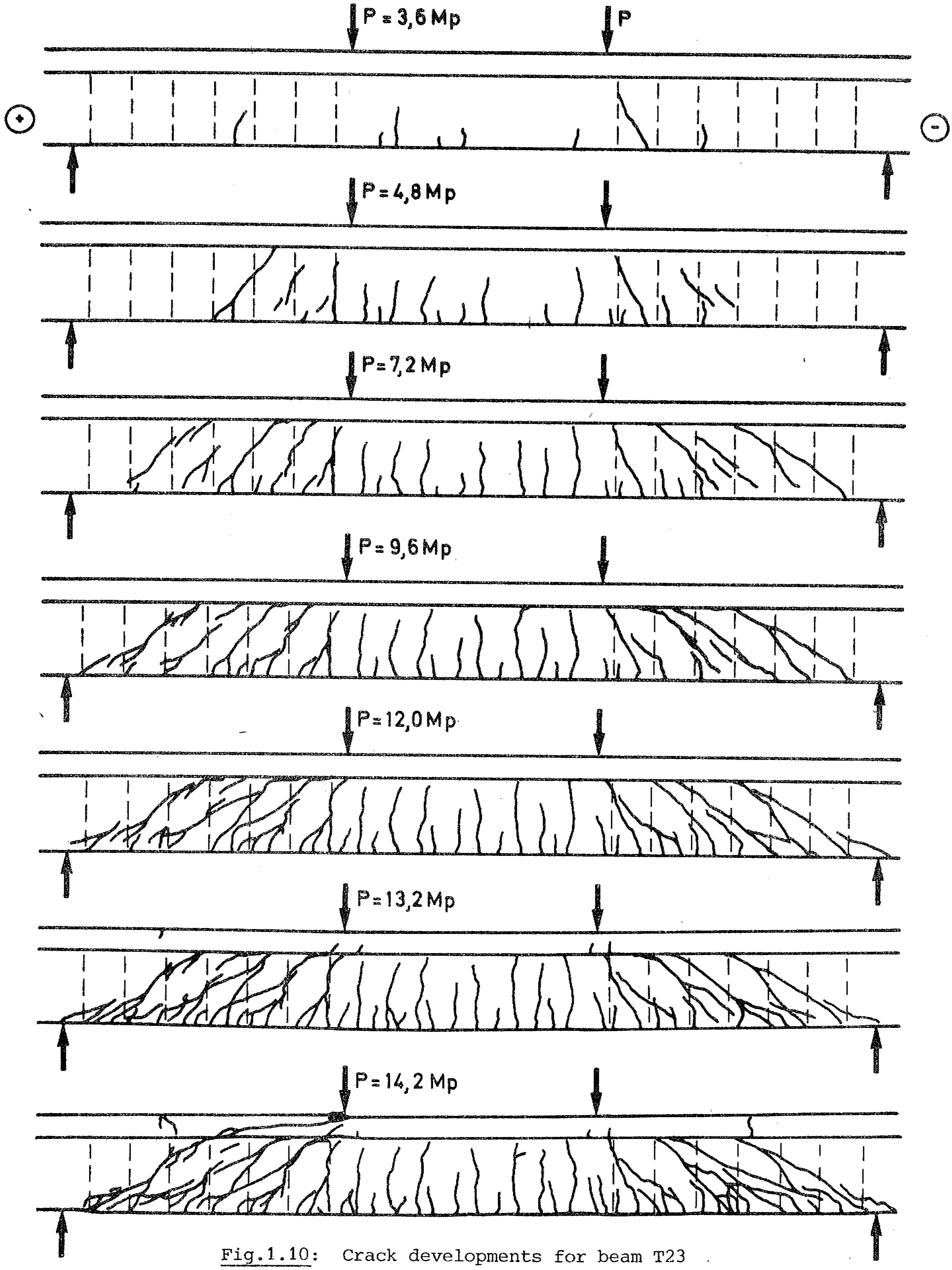

Fig.1.10: Crack developments for beam T23 (side N)

fore failure to see on which side this would occur.

The diagonal crack load P_{cr} defined as the load at which a diagonal crack reached the center line of the beam cross-section can be determined by the following expression in accordance with Zsutty's extended formulae (Zsutty [70.1]):

$$P_{cr} = 10.1(f_c \ \rho_{so} \ \frac{d}{a})^{1/3} \ b_w d \leq 0.93 \sqrt{f_c} \ b_w d \qquad (1.12)$$

Introducing $f_c = 330$ kp/cm² for series I and $f_c = 250$ kp/cm² for series II, we find that

$$P_{cr} = 4.6 \text{ Mp } (v_{cr} = 14 \text{ kp/cm}^2) \text{ for series I}$$

and (1.13)

$$P_{cr} = 4.9 \text{ Mp } (v_{cr} = 15 \text{ kp/cm}^2) \text{ for series II,}$$

which is in excellent agreement with the test results (cf. Fig. 2.9).

1.4 Conclusion

1) A Comparison of the shear failure load of the beams with two typical formulae shows that there is relatively good agreement with Hillerborg's formulae, whereas calculation in accordance with ACI's formulae results in values that are about 60% under the ultimate load of the beams.

2) The crack pattern and measurements with strain-gauges on the concrete compression flange show that a significant arch action develops in the shear span of the beam.

3) Measurements with strain-gauges on the longitudinal reinforcement show that from about 60% of the failure load and up to failure, there is a considerable dowel action.

4) Measurements with strain-gauges on the stirrups show that, in several cases, these reach strain in excess of 0.5%

before failure. In view of this and the results of the measurements of crack widths in the shear span, it should be possible to use stirrups with a yield strength of 5-6000 kp/cm^2 as shear reinforcement.

5) Dial gauge measurements on the outside of the concrete, at a level with the longitudinal reinforcement, result in values that are, at maximum, about 10% too low, compared with the values achieved by means of strain-gauge measurements. The best agreement is obtained when there is no local curvature (dowel action) along the main reinforcement.

1.5 References

[62.1] ACI-ASCE Committee 326:
Shear and Diagonal Tension.
ACI-Journal. Proceedings V. 59, No.1,2,3, 1962, pp.1-30, pp.277-333, pp.353-395.

[63.1] Leonhardt, F., Walther, R.:
Schubversuche an Plattenbalken mit unterschiedlicher Schubbewehrung.
Deutscher Ausschuss für Stahlbeton, H.156, 1963, 84 pp.

[67.1] Özden, K.:
An Experimental Investigation on the Shear Strength of Reinforced Concrete Beams.
Technical University of Istanbul, 1967, 249 pp.

[68.1] Regan, P.:
Shear Strength of Reinforced Concrete Beams.
Department of Civil Engineering, Imperial College, London, 1968, 164 pp.

[68.2] Zsutty, T.C.:
Beam Shear Strength Prediction by Analysis of Existing Data.
ACI-Journal. Proceedings V. 65, No.11, 1968, pp.943-951.

[69.1] Kani, G.N.J.:
A Rational Theory for the Function of Web Reinforcement.
ACI-Journal. Proceedings V. 66, No.3, 1969, pp.185-197.

[69.2] Sørensen, H.C.:
Vejledning i brug af ALGOL-programmerne "SOLARTRONDATA" og "SOLARTRONSTRIMMEL UD".
Del I: Rapport. Del 2: Bilag.
Laboratoriet for Bærende Konstruktioner, DTH, 1969.
25 pp. + bilag.
(Two Computer-programmes)

[70.1] Sørensen, H.C.:
Forskydningsarmering i jernbetonbjælker.
(Web Reinforcement in Reinforced Concrete Beams)
(Danish version of this report),
Tech. University of Denmark, Structural Research Laboratory, Report No.19, 1970, 122 pp.

[71.1] Sørensen, H.C.:
Forskydningsforsøg med 12 jernbetonbjælker med T-tværsnit
(Danish version of this report,
Tech.University of Denmark,Structural Research Laboratory, Report No.20, 1971, 49 pp.

[73.1] CEB
Bulletin d'information no.96, "Notations-Terminologie".
Paris 1973, 159 pp.

[74.1] Sørensen, H.C.:
Efficiency of Bent-up Bars as Shear Reinforcement,
ACI, SP-42-(12) Shear in Reinforced Concrete, 1974,pp. 267-283.
(or. TUD,SRL. Report R.35, 1973)

2. TEST SPECIFICATIONS AND RESULTS

2.1 Beams

2.1.1 Production of beams

Each beam was cast in a steel form, the sides of which were removed 24 hours after casting, after which the beam was covered with wet sachs for 4 days. For the last 9 days, the beam was stored in the laboratory, where the relative humidity was about 50% and the temperature about 18^{o}C. All beams were tested 14 days after casting. The dimensions of the beam and the arrangement of the reinforcement deviated a maximum of ±1 mm from the specifications.

Together with each beam, a number of 15 cm diameter × 30 cm test cylinders were cast, which were stored under the same conditions as the beam. In series I, ten cylinders were cast for each beam, and in series II, six cylinders.

2.1.2 Concrete

Portland high early strength cement ("Rapid") was used for the concrete. For all beams the w/c-ratio was 0.71, and the Webe equal to about 8 sec. The slump was about 1-2 cm. The aggregates used were concrete sand and sea stone in the ratio 35:65. Fig.2.1 shows the sieve analysis for these two materials.

In series I, four cylinders were used to determine the splitting strength of the concrete f_{sp}, and six cylinders to determine the compression strength f_c. Three of the compression cylinders were loaded to failure at a loading rate of about 25 kp/cm^2 per min. The remaining three were loaded to failure at a loading rate of about 6 kp/cm^2 per min. and these were used at the same time for determination of the stress-strain curve for the concrete. For this purpose, two strain-gauges (type, see Section 2.3.2) were placed along two opposite generatrices (ε_1) and two stran-gauges perpendicular to these (ε_2).

In series II, four cylinders were loaded to failure at a loading rate of about 25 kp/cm^2 per min. The other two cylinders were

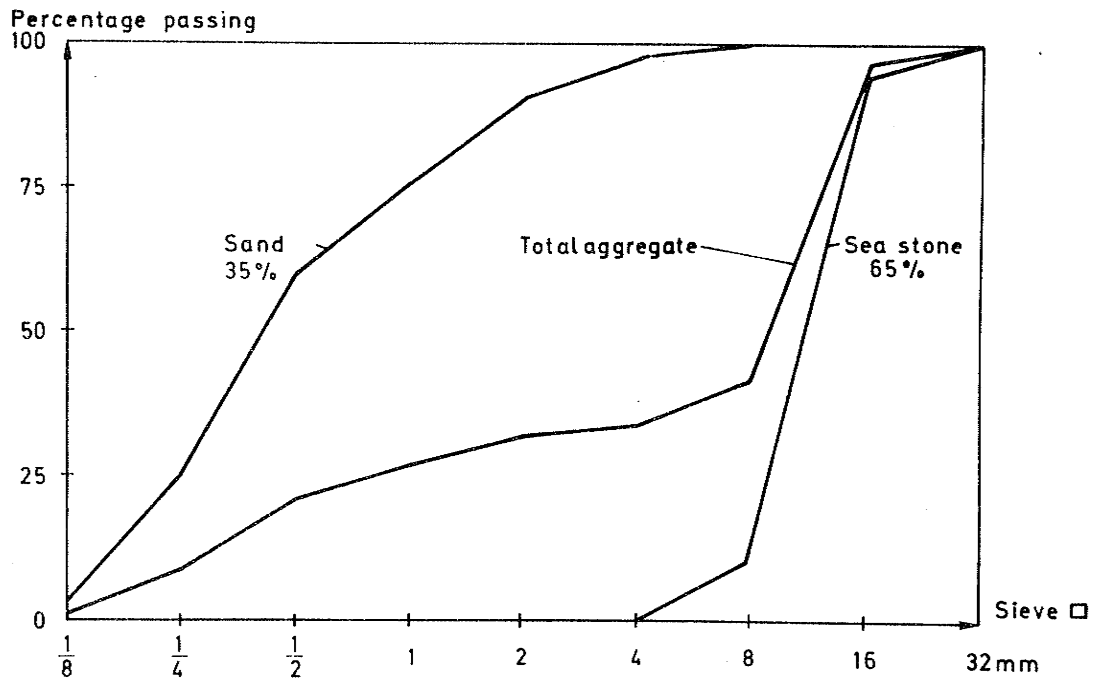

Fig.2.1: Sieve analysis for concrete

loaded to failure at a loading rate of about 9 kp/cm² per min., and were at the same time used for determination of the compressive stress-strain curve of the concrete.

For series I, the compressive strength f_c lay in the interval from 306 to 357 kp/cm², and for series II, in the interval from 209 to 286 kp/cm². The coefficient of variation within each casting was maximum 5%. The average value of f_c for the individual beams is given in table I (Section 1.3.1). The average strength f_{sp} was found to be 34.7 kp/cm² for series I.

Fig.2.2a shows two compressive stress-strain curves for each of the series I and II, corresponding to minimum and maximum f_c. Fig.2.2b shows Poisson's ratio for two cylinders from series I.

Despite identical proportioning in the two test series, it will be seen that f_c in series II deviated significantly from f_c in series I. This difference is probably due to the fact that the cement used came from two different batches.

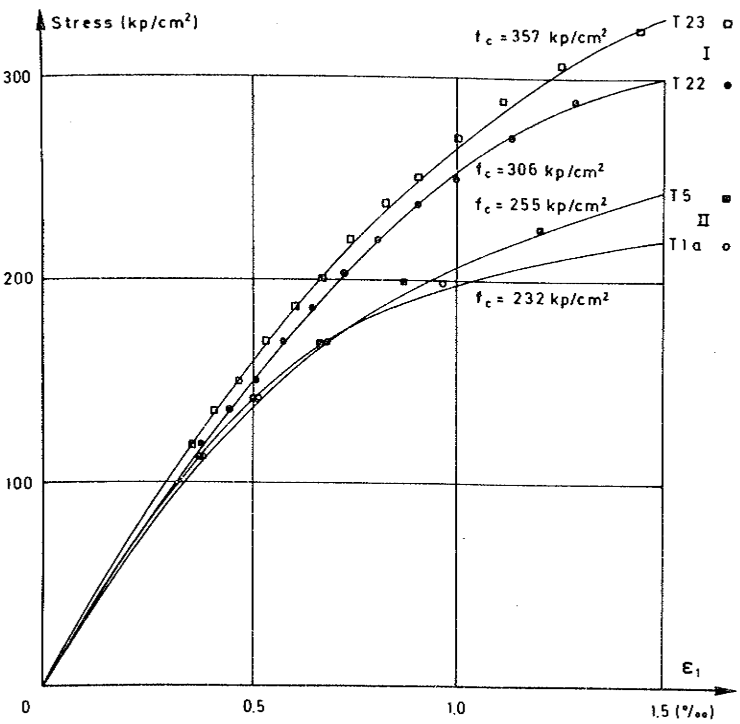

Fig.2.2a:

Compressive stress-strain curves for concrete in series I and II

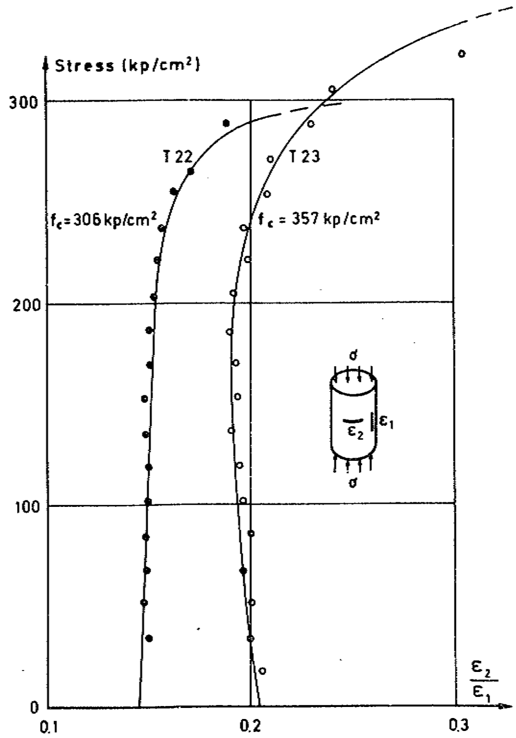

Fig.2.2b:

Poisson's ratio for the concrete in series I

2.1.3 Longitudinal reinforcement in tension flange

A total of 4 no.K.20 Danish kamstål (20 mm dia. deformed, hot rooled bars) in two layers comprised the main reinforcement, resulting in a total nominal area of reinforcement of $A_s = 12.6 \text{cm}^2$. The arrangement of the reinforcing bars is shown in Fig.2.3 and 2.4.

The two reinforcing bars in each layer were cut from the same length of bar, and in addition, a test bar was cut from this for determination of the tensile stress-strain curve. Fig.2.5 and 2.6 show typical stress-strain curves. The figures also give the average value yield stress (f_{sy}) and the modulus of elasticity (E) , together with the coefficients of variation δ (in series I, determined on the basis of six specimens, and in series II, on the basis of 18 specimens). The uniformly distributed elongation

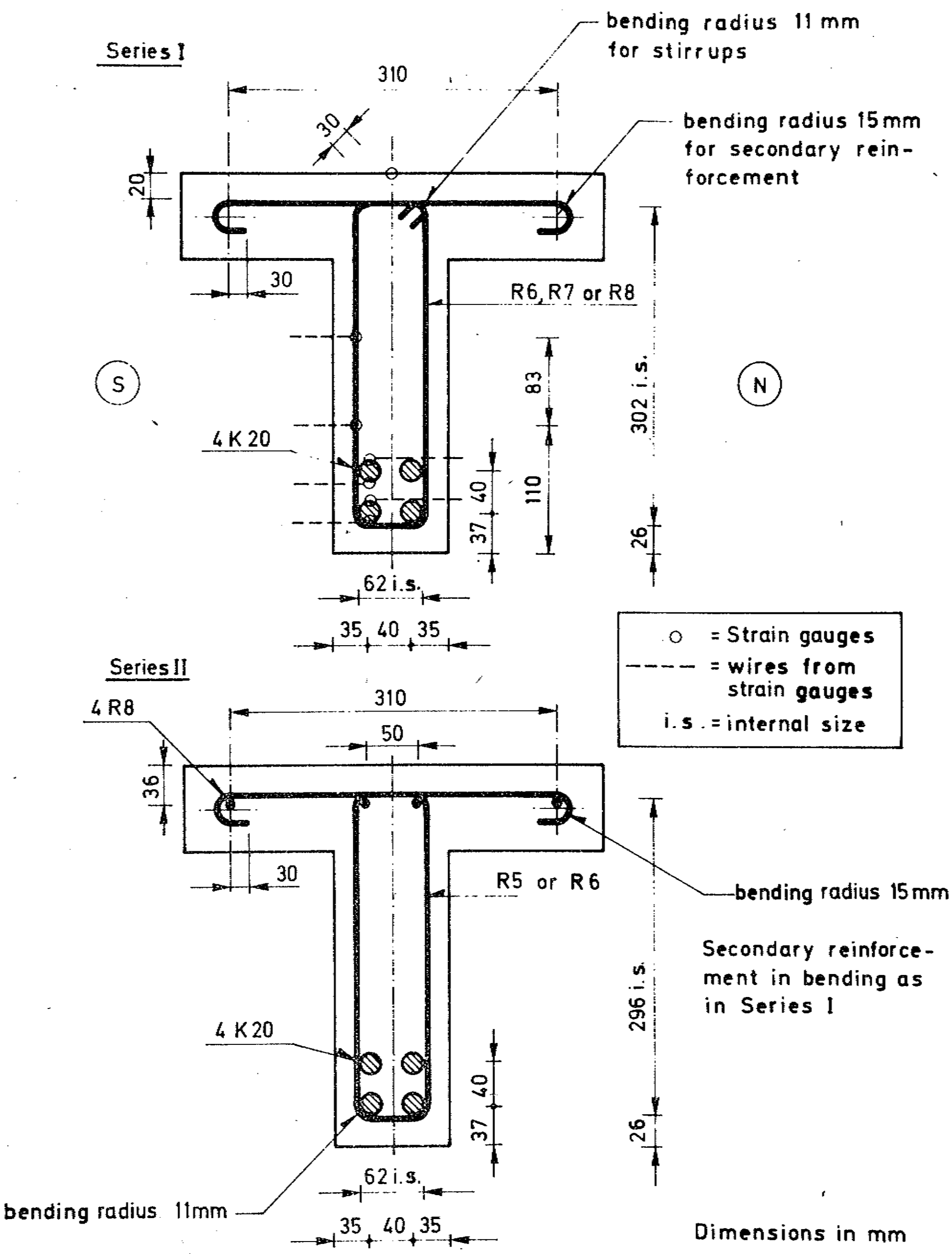

Fig.2.3: Cross section of beams in series I and II. Locations of strain-gauges for beams in series I.

distributed elongation at rupture (ε_u) and the ultimate strength (f_{su}) are also shown in the figures.

2.1.4 Longitudinal reinforcement in compression zone

The beams in series II were provided with longitudinal reinforcement in the compression zone consisting of a total of 8 mm dia. plan mild bars (R8), resulting in a total nominal reinforcing area in the compression zone of 2.01 cm² . The arrangement is

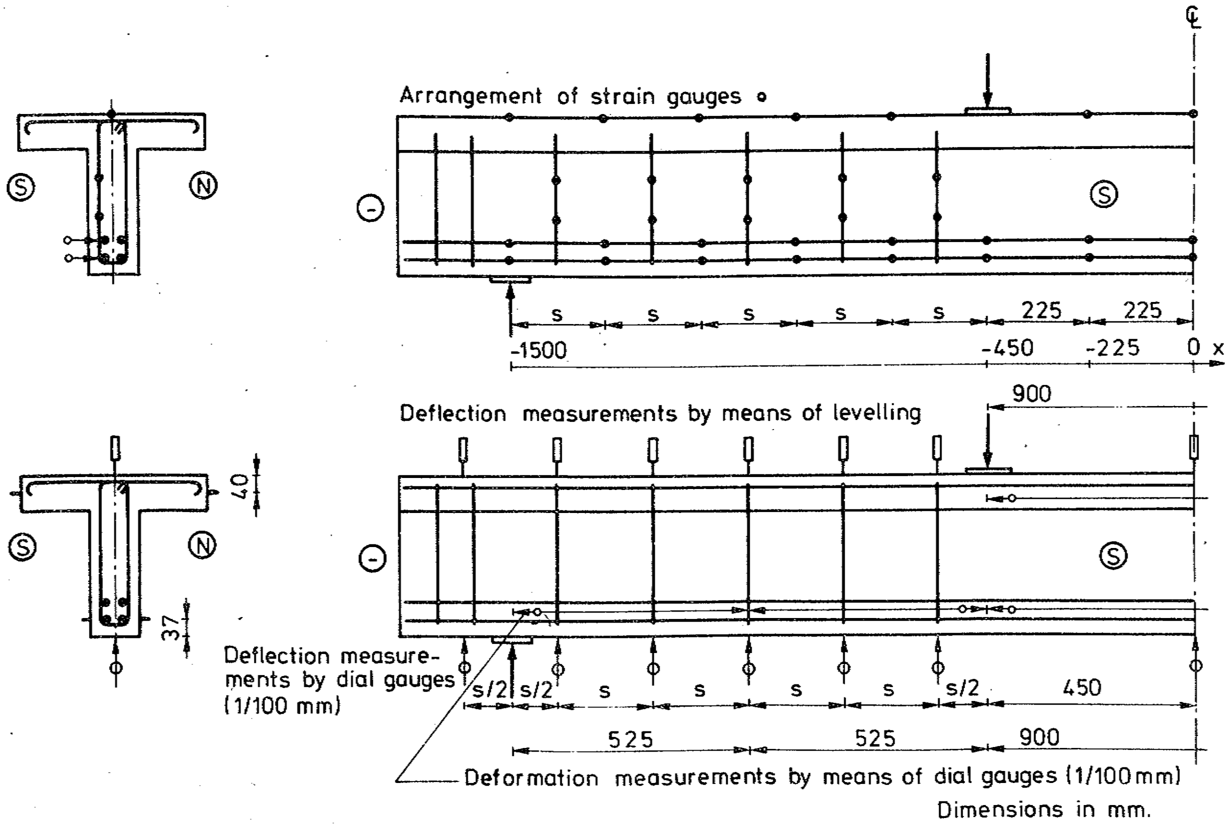

Fig.2.4: Arrangement of reinforcement of beams in series I and II

shown in Fig.2.3 and 2.4. Fig.2.6 shows a typical stress-strain curve for this reinforcement. The figure also shows the yield stress, ultimate strength, modulus of elasticity (E) and elongation at rupture (ε_u) .

2.1.5 Secondary reinforcement in compression flange

In series I, the secondary reinforcement in the compression flange of the beam consisted of 8 mm, dia., plain mild bars (R8) placed perpendicular to the axis of the beam at intervals of 11 cm. The arrangement and shape are shown in Fig.2.3 and 2.4. This reinforcement was of the same type as the stirrup reinforcement used in beam T21.

In series II, the secondary reinforcement consisted of plain

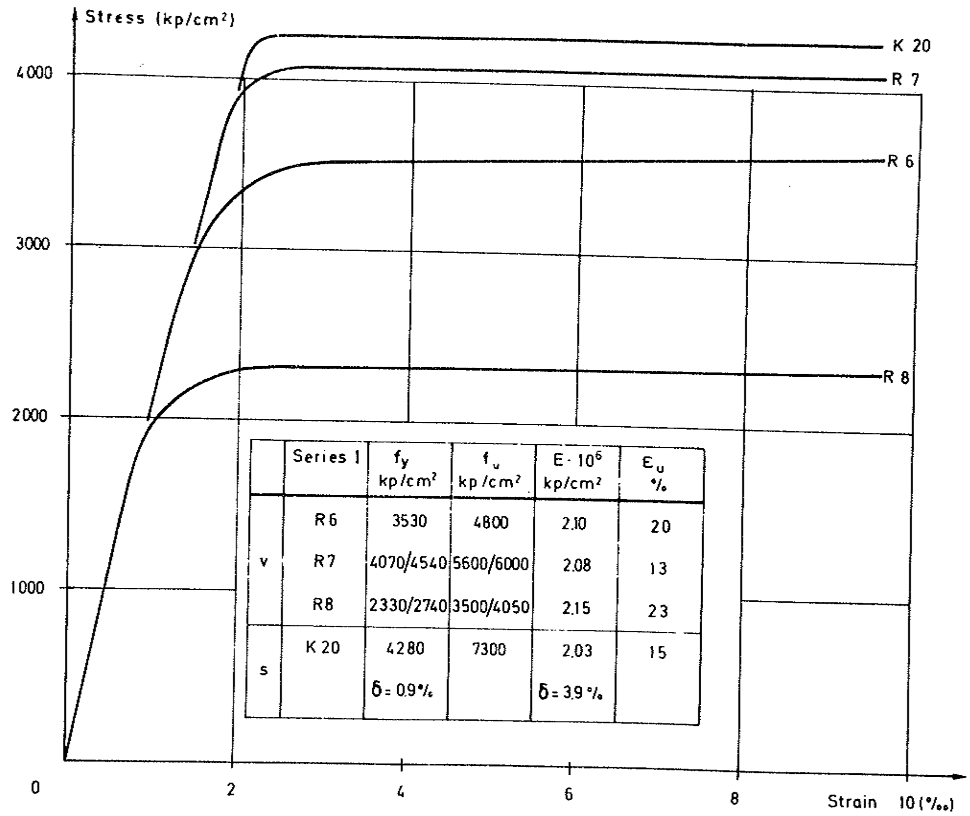

	Series I	f_y kp/cm²	f_u kp/cm²	$E \cdot 10^6$ kp/cm²	ε_u %
v	R 6	3530	4800	2.10	20
	R 7	4070/4540	5600/6000	2.08	13
	R 8	2330/2740	3500/4050	2.15	23
s	K 20	4280	7300	2.03	15
		δ = 0.9 %		δ = 3.9 %	

Fig.2.5: Stress-strain curves for reinforcement in series I

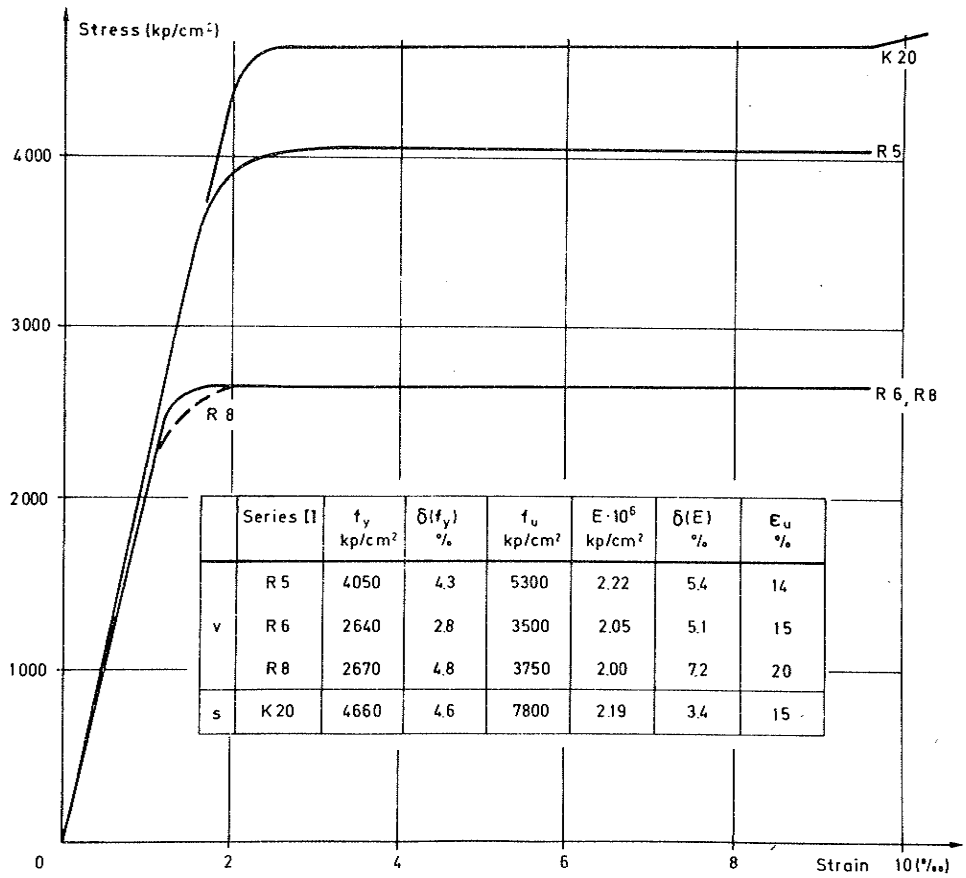

	Series II	f_y kp/cm²	$\delta(f_y)$ %	f_u kp/cm²	$E \cdot 10^6$ kp/cm²	$\delta(E)$ %	ε_u %
v	R 5	4050	4.3	5300	2.22	5.4	14
	R 6	2640	2.8	3500	2.05	5.1	15
	R 8	2670	4.8	3750	2.00	7.2	20
s	K 20	4660	4.6	7800	2.19	3.4	15

Fig.2.6: Stress-strain curves for reinforcement in series II

mild 5 or 6 mm dia. bars (R5 or R6) at intervals of 11 cm in the bending span, the size of the bars being the same as that of the stirrups in the shear span.

2.1.6 Web reinforcement

The web reinforcement consisted of stirrups of plain, mild bars, dia. 5, 6, 7 and 8 mm (R5, R6, R7 or R8). The shape and arrangement of the stirrups are shown in Fig.2.3 and 2.4. The tensile stress-strain diagram for the reinforcement was determinated on the basis of one or two specimens taken from each reinforcing bar. Typical stress-strain curves are shown in Fig. 2.5 and 2.6.

In series I, one of the bars was tested at periods of 2, 2½ and 3 months prior to testing of the relevant beam, while the remaining bars were tested at periods of 1½, 1 and ½ month after testing of the relevant beam, corresponding to the order 7, 8 and 6 mm dia. bars (T22, T21 and T23). For the 7 and 8 mm dia. bars, considerably higher yield strengths were found in the second test than in the first, as will be seen from Fig.2.5. This was presumably due to the fact that the bars had been subjected to final processing in the form of cold-working by the supplier, e.g. a straightening process. The final strength properties of the material are then first reached after a maturation period. The yield strength of the web reinforcement on the day of testing is thus not clearly defined for beams T21 and T22.

In series II, tensile specimens were taken one month before the time of testing and on the test day itself. In this series, no difference in the yield strength was found between the two sets of tests. About 25 single specimens were taken from each type of reinforcement for determination of the stress-strain diagram.

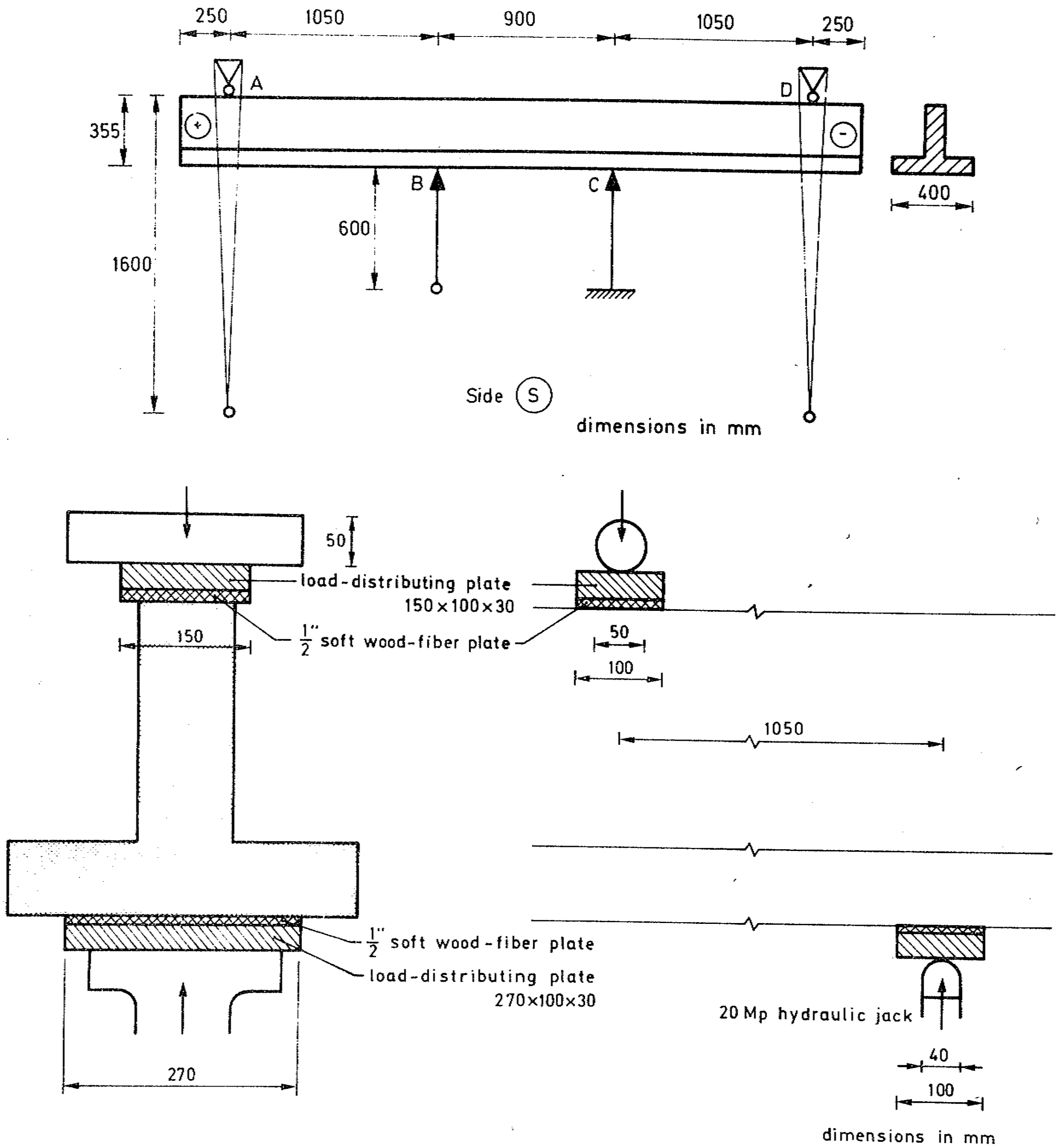

Fig.2.7: Loading arrangement

2.2 Loading

2.2.1 Loading arrangement

The beams were tested in the laboratory's 105 Mp hydraulic flexural testing machine (Amsler), with the compression flange at the bottom, see also Fig.2.7. The hydraulic jack at point C was prevented from moving in the longitudinal direction of the beam, while that at point B could rotate about a point approximately 600 mm below the point of application of the load.

The bearings at point A and D were pendulum bearings with a pendulum arm of about 1600 mm. At jacks B and C, the load was transmitted through two $10 \times 27 \times 3$ cm steel plates, and at bearings A and D, through two $10 \times 15 \times 3$ cm steel plates. At each point, a ½" soft wood-fibre plate was placed between the steel plate and the concrete.

2.2.2 Loading history

In series I, the first five loading stages each had a duration of about 20 min., while the other loading stages each had a duration of about 30 min. The readings given in the tables were taken about 12 min. after application of each load as continuous measurements showed that the strain in the strain-gauges did not become constant until this point.

In series II, each loading stage had a duration of 7 min. (although only 4 min. for beam T5). The dial gauges were read 6½ min. after application of each load (results from series I showed that the dial gauges gave a constant reading 5 min. after loading).

In both series, each loading stage was of the order of magnitude of 1.0 to 1.5 Mp, as shown in the tables in Section 2.3. The load was applied in steps of about 0.2 Mp, and the load was not increased until the dial gauges showed a constant reading at each stage.

2.3 Test results

2.3.1 Strain-gauge measurements, general

All strain-gauges were read automatically by means of two data-loggers (make: Solartron), the readings being taped with a view to computer processing. As a check, the readings were also registred on a printer. A single reading of the total of 100-130 strain-gauges took 90 sec. At each loading stage, the gauges were read 1, 4, 7 and 10 min. after application of the load. After the 10-minute reading, the gauges were read automatically at 90 sec. intervals. In this way, a total of 7-8 readings were taken at each loading stage.

An examination of the about 7 readings at each stage showed that while the strain in the reinforcement remained in the elastic range, a stable state of strain occurred with 4-7 minutes. When the strain in the reinforcement exceeded the elastic range, only insignificant changes occurred after about 12 min. In the tables the strain is therefore given for the 5th reading (about 12 min. after application of the load).

The basic computer processing (control of correct punching, temperature compensation and zero-correction) was carried out by means of the laboratory's two standard programmes (Sørensen [69.2]).

The resolving power (including zero-point movement) of the measuring equipment was about 8×10^{-6} mm/mm , which is higher than the accuracy of the strain-gauges (about 2×10^{-6}mm/mm).

2.3.2 Strain along concrete compression flange (series I)

85 mm strain-gauges (600 Ω single-wire) were placed along the center line of the surface of the compression flange. The arrangement is shown in Fig.2.8. The strain-gauges, incl. glue, are linear for strain of less than 0.3%.

2.3.3 Strain along longitudinal reinforcement (series I)

6 mm strain-gauges (type HBM 6/120 LE 11) were placed in a number of sections perpendicular to the axis of the beam on the two longitudinal reinforcing bars in side S . The arrangement of the measuring sections aimed at is shown in Fig.2.8. Four strain-gauges were placed in each cross-section, see Fig.2.3. In order to ensure that the strain-gauges stayed put, one bit on each side of the reinforcing bar was ground away, see Fig.2.9. The positions of the strain gauges deviated a maximum of ±5 mm from the intended positions. The strain-gauges used (incl.glue) are linear for strain not exceeding 0.7% .

During the 14 days from casting of the concrete to execution of the test, a regular check was made on the insulation resistance

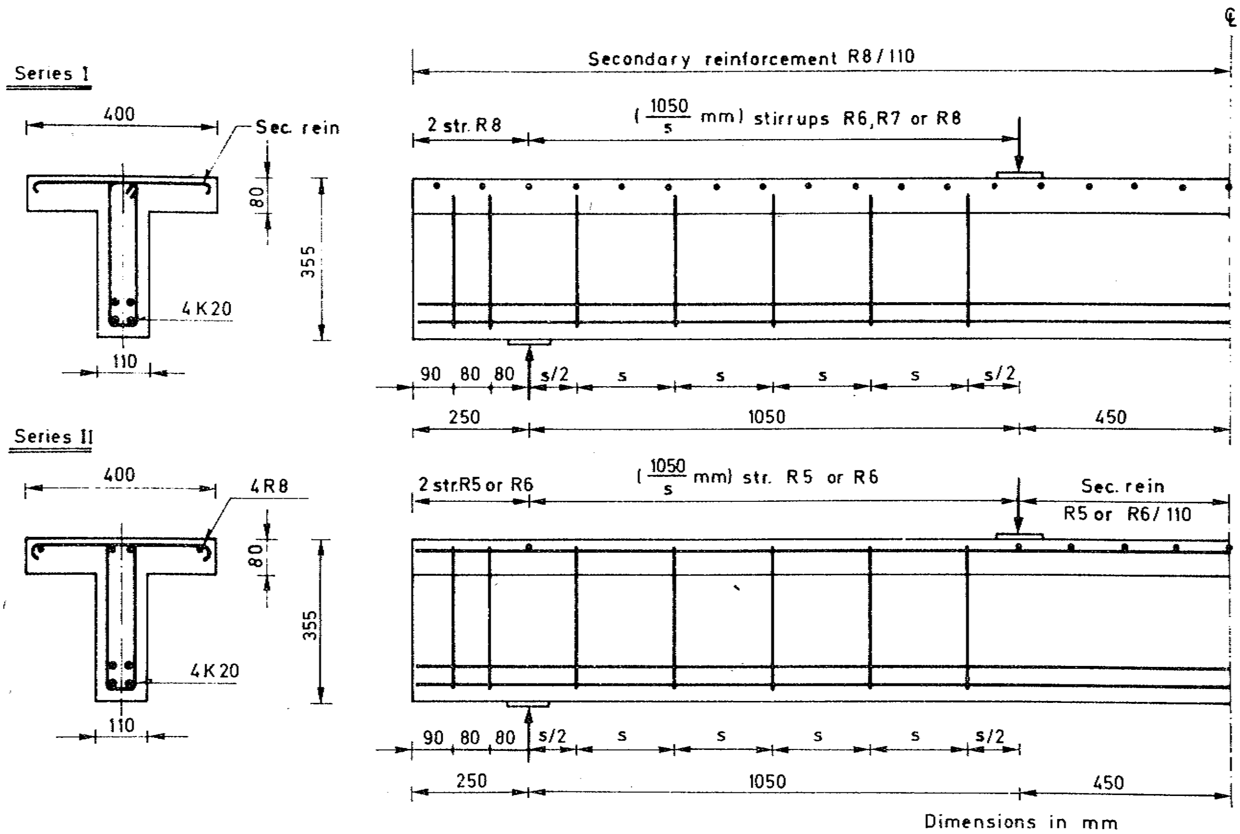

Fig.2.8: Locations of measuring points for beams in series I

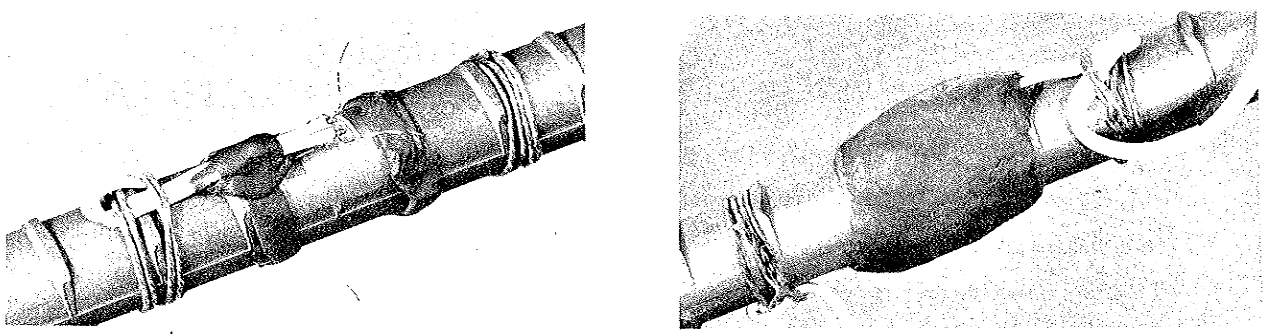

Fig.2.9: Strain-gauges on 20 mm bar, - with and without moister protection

of the strain-gauges. It was found that 1-6 strain-gauges in each beam had too low an insulation resistance and these had to be left out of account.

Table IIIa-c shows the strain registered by each strain-gauge for the three beams in series I. For beam T23, Fig.1.4 shows the development of the force (N_s) along the beam, and Fig.1.9 shows the average strain along the beam in the bottom reinforcing bar, for comparison with the results of the dial gauge measurements.

2.3.4 Strain in stirrups (series I)

Two 6 mm strain-gauge (type HBM 6/120 LE 11) were placed on each stirrup in the bending span. The gauges were placed on the stirrup-leg in beam side S . The arrangement of the strain -gauges is shown in Fig.2.3.

Table IVa-c gives the strain for the three beams in series I. Near failure, the strain became so great in several cases that the measurement range was exceeded (or the strain-gauge wires broke). Fig.1.7 shows the development of strain in four stirrups in beam T23.

2.3.5 Deflection measurements (series I)

Deflection measurements were carried out on the beams in series I, on the tensile side by means of 1/100 mm dial gauges, and on the compression side by levelling. The locations of the measuring points are shown in Fig.2.8. The displacements given in table Va-c are calculated from the line connecting two points at a distance $\pm(1500\text{ mm} + \frac{1}{2}s)$ from the middle of the beams. The inaccuracy on the displacements thus calculated is ±0.3mm. Fig.1.8 shows the deflection of beam T23 at various loading stages.

2.3.6 Measurements with dial gauges

In series I, deformation measurements were taken along the bottom layer of the longitudinal reinforcement and along the middle of the concrete compression flange in the bending span, see also Fig.2.8. The measurements were taken by means of 1/100 mm dial gauges. Table VIa-c gives the average strain calculated on the basis of the measurements. Fig.1.9 shows a comparison of the measurements with dial gauges with those taken with strain-gauges.

In series II, the deformations were only measured in the middle span - partly along the center-line of the longitudinal reinforcement, and partly along the concrete compression flange, at about the level of the compressive reinforcement. Table VII shows the resultant average strain.

2.3.7 Cracking and crack widths

At each loading stage the cracks formed were mapped and numbered; the numbering was carried out by drawing a line across the ends of the cracks after each loading stage and marking this line with the number of the loading stage. The relationship between the crack number and the load appears from tables VI and VII in Section 2.4. Fig.2.10a-n shows the crack pattern immediately after failure for all beams, seen from the S-side.

Fig.1.10 in Section 1.3.7 depicts the development of cracking at a number of loading stages for beam T23, seen from the N-side. Table VII gives the maximum crack widths for the beams in series I at a few loading stages.

2.4 Tables II-XIII, Fig.2.10

Table IIa. T21: Strain along compression flange, strain-gauges.

x \ P	1.3	2.6	3.9	5.2	6.5	7.8	9.1	10.4	11.7	13.0
0	-87	-175	-274	-376	-480	-585	-701	-819	-947	-1079
-225	-87	-182	-289	-397	-507	-622	-753	-890	-1046	-1205
225	-85	-175	-275	-381	-487	-597	-720	-842	-978	-1113
-660	-64	-126	-216	-310	-364	-438	-507	-585	-651	-630
660	-66	-130	-213	-281	-377	-457	-532	-571	-603	-608
-870	-47	-94	-121	-147	-145	-246	-291	-274	-201	42
870	-9	-102	-123	-168	-242	-317	-331	-329	-305	-251
-1080	-28	-61	-85	-78	-88	-23	12	54	125	468
1080	-28	-55	-80	-87	-54	-29	12	68	161	398
-1290	-12	-23	-35	-36	-24	31	55	83	123	185
1290	-10	-21	-31	-9	10	28	52	76	104	149
-1500	2	5	9	12	23	47	68	99	137	158
1500	5	9	12	16	29	48	71	97	135	199

Table IIb. T22: Strain along compression flange, strain-gauges.

x \ P	0.2	1.2	2.4	3.6	4.8	6.0	7.2	8.4	9.6	10.8	12.0	13.2
0	-3	-61	-149	-234	-326	-414	-507	-603	-698	-802	-907	-1013
-225	-2	-54	-132	-206	-287	-365	-448	-537	-629	-732	-845	-965
225	-2	-59	-142	-218	-303	-395	-488	-589	-687	-800	-914	-1034
-625	-2	-43	-106	-166	-237	-310	-390	-469	-544	-627	-687	-1441
625	-2	-45	-109	-173	-260	-350	-438	-500	-573	-625	-634	-634
-800	-2	-35	-83	-130	-180	-251	-305	-357	-407	-440	-407	-327
800	0	-50	-123	-173	-206	-253	-291	-384	-423	-454	-474	
-975	-2	-29	-68	-107	-125	-178	-218	-206	-242	52	-194	-64
975	-3	-29	-68	-102		-87	-194	-178	-175	-152	213	36
-1150	0	-28	-50	-71		-55	-52	-29	12	100	320	1035
1150	0	-17	-42	-64	-64	-66	-68	-19	10	68	156	222
-1325	0	-19		-35	-35	-5	12	33	69	90	118	215
1325	0	-24		-40	-43	-21	-3	40	59	78	99	133
-1500	2	-2	3	5	7	21	33	45	62	81	113	126
1500	0	5	3	7	12	21	38	61	81	104	121	149

Table IIc. T23: Strain along compression flange, strain-gauges.

x \ P	0.2	1.2	2.4	3.6	4.8	6.0	7.2	8.4	9.6	10.8	12.0	13.2	14.2
0	-5	-59	-140	-222	-310	-398	-487	-574	-669	-765	-867	-977	-1103
-225	-3	-59	-140	-227	-315	-407	-499	-590	-694	-795	-908	-1040	-1167
225	-5	-59	-142	-223	-312	-403	-500	-598	-707	-821	-946	-1087	-1214
-600	-3	-50	-121	-173	-258	-369	-494	-605	-699	-836	-984	-1050	-1191
600	-3	-50	-113	-180	-275	-362	-452	-524	-617	-771	-810	-941	-1075
-750	-3	-40	-92	-139	-190	-199	-246	-302	-330	-303	-243	-96	-111
750	-3	-40	-97	-151	-204	-241	-272	-313	-371	-358	-326	-385	-464
-900	-3	-33	-76	-119	-133	-197	-227	-247	-335	-310	-240	-84	-17
900	-3	-33	-76	-113	-130	-218	-327	-366	-392	-348	-316	-276	-272
-1050	-2	-23	-54	-87	-118	-128	-137	-138	-86	-29	49	233	706
1050	-2	-23	-48	-73	-85	-85	-59	-29	10	99	224	927	1046
-1200	-2	-16	-36	-54	-61	-43	-23	-3	39	78	134	288	532
1200	-2	-14	-31	-48	-61	-12	2	22	42	76	119	226	232
-1350	-3	-9	-14	-17	-23	3	24	42	65	87	110	146	369
1350	-2	-9	-14	-21	-28	0	16	32	51	76	101	134	165
-1500	0	2	3	7	9	21	35	49	67	85	106	127	178
1500	-2	-2	2	3	3	14	26	42	63	88	119	103	109

P in Mp, exclusive of weight of beam 0.15 Mp/m
x in mm. Strain in 10^{-6} mm/mm

Table IIIa: T21. Strain in longitudinal reinforcement

x		1.3	2.6	3.9	5.2	6.5	7.8	9.1	10.4	11.7	13.0
0	1	220	438	685	928	1166	1395	1634	1874	2105	2098
	2	207	402	616	829	1039	1246	1468	1686	1923	2069
	3	184	358	553	746	936	1123	1324	1522	1724	2015
	4	132	283	544	612	771	989	1108	1284	1472	1709
-225	1	145	402	645	878	1118	1351	1598	1841	2090	2211
	2	151	396	633	846	1060	1269	1493	1713	1939	2189
	3	128	331	534	725	921	1108	1307	1504	1707	1927
	4	121	318	517	693	865	1033	1211	1389	1573	1778
225	1	186	379	630	875	1116	1349	1594	1837	2084	2149
	2	153	329	582	808	1024	1234	1455	1675	1904	2193
	3	151	316	534	731	928	1120	1321	1520	1722	1956
	4	147	299	511	700	875	1047	1229	1403	1583	1797
-450	1	211	400	632	867	1118	1365	1619	1876	2142	2390
	2	188	366	565	754	942	1125	1321	1514	1719	1966
	3	170	331	530	725	924	1118	1321	1523	1736	1958
	4	176	339	515	676	825	972	1125	1273	1420	1575
450	1	203	400	622	856	1089	1317	1562	1807	2059	2216
	2	199	392	588	794	989	1185	1393	1606	1826	2069
	3	178	343	538	735	932	1118	1315	1510	1703	1918
	4	182	348	526	687	834	976	1125	1275	1432	1611
-660	1										
	2	149	354	576	766	953	1114	1263	1418	1590	1887
	3	117	285	467	635	821	1030	1261	1481	1703	1906
	4	117	276	454	595	737	867	989	1093	1187	1278
660	1	167	364	618	909	1185	1460	1745	2036	2299	2815
	2	136	304	498	685	865	1039	1231	1416	1621	1891
	3	121	270	473	710	928	1148	1353	1566	1782	2011
	4	109	251	425	584	702	794	894	997	1100	1221
-870	1	103	222	400	628	854	1108	1393	1675	2025	2603
	2	103	228	440	622	746	867	978	1081	1175	1403
	3	80	189	358	513	656	790	961	1145	1345	1715
	4	78	182	369	521	687	823	930	1011	1058	804
870	1	92	239	492	731	951	1162	1449	1669	1889	2101
	2	80	199	373	534	731	940	1116	1296	1489	1677
	3	67	163	360	547	785	961	1148	1317	1464	1604
	4	63	165	360	431	509	681	880	1055	1231	1374
-1080	1	34	134	283	482	744	978	1196	1433	1753	2008
	2	38	132	289	492	549	662	762	823	850	911
	3	33	94	214	415	586	660	766	877	1039	1280
	4	29	77	189	423	544	653	766	886	974	1141
1080	1	65	122	232	356	630	811	1062	1347	1734	2180
	2	54	107	216	425	576	708	794	852	834	798
	3	42	88	178	327	488	632	790	965	1240	1466
	4	36	78	199	387	519	676	926	984	951	907
-1290	1	19	38	67	188	387	700	930	1158	1414	1675
	2	21	34	78	235	329	400	427	427	425	362
	3	15	31	52	138	300	528	658	767	905	1129
	4	10	21	38	144	293	465	572	679	758	940
1290	1	19	48	100	268	442	632	884	1099	1330	1541
	2	15	38	82	291	371	402	406	389	383	423
	3	13	29	56	189	274	354	515	679	878	1072
	4	13	34	71	343	545	637	689	723	792	984
-1500	1	-2	-8	-15	-15	-4	40	71	111	144	144
	2	11	21	29	52	98	279	410	568	785	1053
	3	4	8	13	19	36	149	233	331	477	660
	4	10	19	29	40	65	218	341	480	697	1033
1500	1	-6	-10	-15	-11	4	44	94	130	163	184
	2	4	13	25	48	105	226	398	601	798	989
	3	0	6	10	34	61	98	161	245	346	467
	4	11	21	33	52	98	218	344	534	744	984

P in Mp, exclusive of weight of beam 0.15 Mp/m
x in mm. Strain in 10^{-6} mm/mm

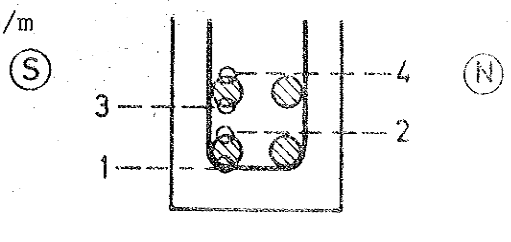

Table IIIb: T22. Strain in longitudinal reinforcement

x		P 0.2	1.2	2.4	3.6	4.8	6.0	7.2	8.4	9.6	10.8	12.0	13.2
0	1	6	132	356	568	781	988	1194	1401	1604	1814	2023	2262
	2	4	113	333	524	718	905	1097	1288	1478	1669	1866	2065
	3	6	96	289	465	651	823	999	1175	1347	1523	1703	1885
	4	6	94	318	482	647	802	963	1122	1278	1439	1602	1768
-225	1	8	84	314	521	741	955	1160	1367	1566	1776	1987	2147
	2	6	96	331	528	725	917	1104	1292	1481	1675	1874	2094
	3	6	82	270	452	635	817	997	1173	1347	1525	1707	1885
	4	4	78	270	431	595	743	901	1062	1219	1384	1548	1713
225	1	8	132	350	553	764	965	1164	1370	1569	1774	1979	2144
	2	10	128	329	517	716	915	1110	1303	1495	1690	1891	2098
	3	8	103	274	442	624	811	988	1164	1338	1514	1694	1874
	4	6	105	293	446	614	790	957	1122	1282	1445	1610	1774
-450	1	8	124	358	563	769	967	1162	1363	1564	1768	1981	2167
	2	15	111	331	517	712	901	1093	1282	1744	1958	2167	2352
	3	6	86	272	444	624	798	974	1150	1322	1497	1671	1837
	4	6	71	272	434	607	773	932	1091	1242	1397	1550	1690
450	1	6	117	323	538	750	953	1160	1367	1571	1789	2006	2168
	2	6	107	312	498	685	869	1058	1242	1424	1611	1801	2008
	3	4	88	287	467	643	813	986	1154	1330	1510	1690	1864
	4	4	71	279	448	595	743	892	1037	1187	1338	1487	1631
-625	1	4	77	270	480	695	894	1095	1298	1499	1707	1929	2121
	2	4	73	258	456	641	810	972	1129	1286	1445	1629	1822
	3	2	63	228	419	616	810	997	1185	1365	1543	1698	1830
	4	4	57	211	389	568	727	875	1018	1150	1277	1382	1462
625	1	6	82	287	492	718	926	1143	1393	1613	1835	2054	2239
	2	6	77	264	459	656	836	1007	1164	1322	1497	1680	1893
	3	4	65	224	396	570	739	917	1127	1300	1460	1613	1761
	4	2	54	189	369	557	733	867	984	1112	1238	1363	1489
-800	1	2	52	149	366	582	777	974	1167	1368	1579	1920	2287
	2	2	54	193	394	557	699	838	980	1118	1261	1372	1502
	3	4	48	138	316	496	658	831	1007	1185	1357	1619	1860
	4	4	40	115	291	498	635	758	857	957	1051	1049	863
800	1	4	56	212	427	643	856	1064	1269	1497	1744	2010	2293
	2	2	59	199	396	567	695	829	986	1133	1296	1466	1671
	3	2	50	163	350	528	720	915	1089	1275	1453	1623	1795
	4	2	48	138	335	469	580	674	789	886	972	1016	1049
-975	1	2	40	122	251	454	630	813	980	1137	1083	1426	1552
	2	-2	34	109	237	385	513	660	811	968	2568	1376	1634
	3	-4	29	92	201	358	473	595	716	827	965	1085	1187
	4	2	31	88	201	371	473	563	660	769	942	1148	1458
975	1	0	17	113	268	905	1167		1041		1474	1763	2676
	2	0	34	107	253	601	452	718	792	921	1014	258	1870
	3	0	29	100	228	373	498	744	857	1039	1223	475	1577
	4	-2	29	82	209	446	567	670	731	844	940	976	875
-1150	1	0	25	67	155	285	434	565	731	907	1154	1851	2289
	2	0	15	54	157	852	513	1376	683	1233	1328	1187	984
	3	0	13	52	124		344	161	568	180	649	844	281
	4	0	2	36	124		394	482	664	754	764	672	557
1150	1	0	15	92	195	664	528	890	896	1122	1215	1284	1409
	2	0	23	80	178	320	423	494	597	697	825	1028	1321
	3	2	21	73	155	310	456	628	769	907	1066	1150	1125
	4	0	17	63	167	300	362	398	421	448	567	957	1487
-1325	1	0	0	17	52	157	331	214	651	808	949	1100	926
	2	8	13	31	52	159	274	270	333	369	425	563	1066
	3	0	8	25	46	122	295	423	559	700	852	972	417
	4	0	10	25	44	151	329	369	362	352	343	584	1724
1325	1	0	11	29	71	167	343	498	649	787	949	1135	1257
	2	2	11	23	50	134	249	310	371	417	448	473	595
	3	0	0	618	46	101	235	645	519	744	773	892	1079
	4	0	0		29	98	272	362	470	555	649	725	917
-1500	1	-2	-4	-6	-8	-10	15	52	84	109	121	119	77
	2	-2	4	10	19	33	80	170	285	419	589	819	1420
	3	-2	2	6	10	15	36	57	86	136	207	323	611
	4	0	6	15	23	33	56	90	144	235	367	597	1173
1500	1	-4	-2	-4	-4	2	21	59	117	161	201	237	268
	2	-4	2	6	11	25	57	126	253	369	530	687	856
	3	-2	2	6	11	21	34	59	134	209	302	404	532
	4	-2	4	10	15	25	33	65	170	281	423	584	810

P in Mp, exclusive of weight of beam 0.15 Mp/m
x in mm. Strain in 10^{-6} mm/mm

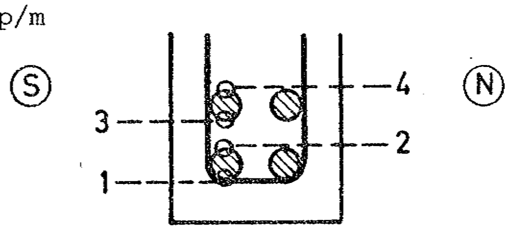

Table IIIc: T23. Strain in longitudinal reinforcement

x		0.2	1.2	2.4	3.6	4.8	6.0	7.2	8.4	9.6	10.8	12.0	13.2	14.2
0	1	6	126	352	576	790	1009	1225	1422	1636	1841	2050	2205	2071
	2	8	113	312	505	697	890	1079	1254	1445	1629	1816	2069	2092
	3	6	92	278	457	633	810	984	1146	1326	1495	1667	1862	2260
	4	21	80	293	467	630	785	938	1078	1234	1382	1531	1853	2046
-225	1	8	107	341	547	760	974	1185	1380	1590	1791	1990	2165	2044
	2	6	94	297	500	697	896	1089	1267	1462	1650	1837	2063	2126
	3	6	71	272	456	633	811	988	1150	1326	1491	1659	1847	2167
	4	6	71	276	438	591	744	894	1032	1183	1326	1474	1640	1897
225	1	6	105	320	538	743	949	1156	1359	1585	1793	2002	2205	2117
	2	11	109	299	492	685	878	1070	1252	1455	1642	1833	2046	2130
	3	4	84	279	467	643	819	997	1164	1347	1518	1686	1872	2092
	4	6	77	233	389	544	702	859	1011	1187	1351	1514	1694	1916
-450	1	-6	124	325	542	731	921	1112	1292	1495	1694	1899	2111	2117
	2	4	105	295	484	670	857	1045	1217	1407	1587	1784	1989	2061
	3	4	88	266	440	612	781	951	1108	1273	1432	1590	1759	1962
	4	4	73	243	379	519	666	817	955	1108	1252	1416	1585	1799
450	1	8	147	356	565	767	974	1175	1363	1573	1774	1979	2199	2396
	2	6	111	306	494	689	877	1060	1234	1426	1610	1799	2000	2040
	3	6	101	279	457	637	808	980	1139	1317	1483	1648	1826	2006
	4	6	84	260	438	624	789	951	1099	1259	1409	1556	1717	1945
-600	1	6	73	295	494	704	919	1129	1332	1566	1780	2008	2245	2371
	2	4	61	256	457	639	810	972	1120	1284	1435	1594	1786	2033
	3	4	59	243	436	611	789	963	1131	1319	1497	1671	1845	2042
	4													
600	1	8	69	266	484	689	888	1091	1286	1500	1717	1943	2147	2056
	2	10	78	264	480	681	880	1066	1238	1426	1608	1791	2010	2113
	3	4	65	230	417	588	756	919	1076	1250	1409	1548	1709	1893
	4	6	61	226	396	568	750	903	1043	1194	1326	1439	1579	1761
-750	1	2	40	232	434	651	838	1007	1158	1382	1571	1767	2008	2149
	2	4	52	209	394	576	741	915	1093	1294	1468	1640	1826	1948
	3	4	48	189	362	526	679	825	947	1100	1246	1382	1506	1627
	4	6	46	180	350	477	595	733	896	1213	1386	1527	1613	1726
750	1	8	52	228	410	630	821	1035	1248	1483	1757	2078	2291	2205
	2	6	56	205	390	599	766	934	1074	1213	1370	1537	1770	1967
	3	4	48	188	337	500	649	829	1005	1200	1376	1554	1728	1948
	4	6	50	172	348	515	649	825	959	1078	1146	1152	1215	1313
-900	1	38	100	211	358	578	815	1018	1202	1424	1665	1929	2498	2924
	2	6	56	157	291	496	614	735	840	947	1055	1160	1215	1382
	3	2	44	140	260	463	632	794	945	1146	1322	1497	1908	2170
	4	4	42	132	243	452	574	670	741	777	798	787	524	406
900	1	4	42	159	335	547	741	944	1139	1349	1598	1765	2017	2126
	2	4	40	149	318	488	614	729	844	974	1131	1347	1518	1633
	3	6	38	134	276	480	639	806	965	1123	1282	1365	1493	1610
	4	0	29	121	291	461	567	653	720	787	865	1106	1145	1164
-1050	1	4	27	98	193	362	555	764	947	1152	1432	1736	1872	2084
	2	2	25	103	211	396	549	656	723	829	871	917	1211	1223
	3	4	27	94	189	339	482	643	798	945	1196	1447	1531	1719
	4	2	21	78	168	329	465	620	727	792	748	691	953	928
1050	1	4	31	86	172	392	595	739	888	1074	1370	1659	2013	2239
	2	4	29	84	178	381	544	670	789	894	949	1024	1053	986
	3	4	29	78	163	377	524	630	739	894	1156	1326	1567	1826
	4	4	29	71	161	373	475	570	666	762	756	796	794	744
-1200	1	4	23	63	144	256	457	591	706	861	926	940	1087	1171
	2	2	19	59	144	272	408	509	609	723	921	1177	1365	1433
	3	2	17	52	121	239	390	496	605	735	842	852	1035	1202
	4	2	13	42	103	233	360	408	450	509	722	1122	1441	1569
1200	1	4	21	46	82	218	501	649	794	938	1024	1137	1332	1523
	2	6	21	46	90	228	415	503	588	702	938	1087	1150	1056
	3	4	19	42	78	153	379	494	622	760	936	1085	1282	1564
	4	6	17	38	71	170	270	302	346	436	697	932	1099	1087
-1350	1	0	8	21	31	124	297	467	599	756	945	1148	1367	1284
	2	2	8	19	29	109	310	337	352	371	377	373	411	767
	3	0	4	15	23	84	216	344	427	515	614	773	988	970
	4	2	6	13	17	78	333	452	534	641	712	769	953	1537
1350	1	0	11	27	38	65	186	268	348	463	597	737	892	641
	2													
	3	2	10	19	36	59	186	278	358	448	576	729	854	674
	4													
-1500	1	6	-6	-11	-29	-34	-27	4	34	61	61	36	-57	-82
	2	4	4	11	11	27	61	168	308	494	679	898	1192	1460
	3	8	6	10	10	21	48	92	144	230	299	373	480	628
	4	10	6	11	15	29	54	115	197	364	526	723	1064	1424
1500	1	4	-6	-10	-23	-21	-6	23	63	109	136	144	103	144
	2	6	4	10	6	13	42	109	237	402	586	769	1053	1280
	3	6	2	8	2	11	36	71	115	180	253	335	446	559
	4	4	6	13	11	23	52	121	235	390	580	798	1150	1464

P in Mp, excl. of weight of beam 0.15 Mp/m
x in mm. Strain in 10^{-6} mm/mm

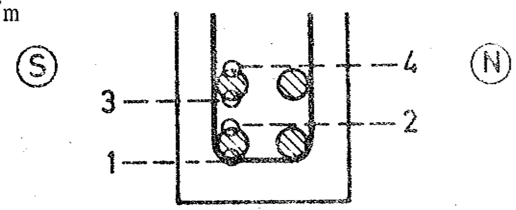

Table IVa: T21. Strain in stirrups

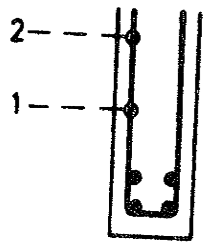

x \ P		1.3	2.6	3.9	5.2	6.5	7.8	9.1	10.4	11.7	13.0
-550	1	-2	2	19	48	96	182	344	500	695	871
	2	-2	36	163	253	369	538	775	961	1185	1361
550	1	-6	17	67	90	128	220	371	521	685	844
	2	-6	-15	19	101	211	331	505	689	880	1055
-765	1	-4	4	115	318	599	878	1208	1569	1885	1952
	2	6	21	270	526	829	1100	1411	1856	3514	
765	1	-13	-27	17	100	299	679	1064	1359	1724	1899
	2	4	19	61	140	293	492	863	1167	1638	1768
-975	1	11	0	98	505	850	1041	1309	1860	5332	
	2	10	-6	33	383	706	951	1211	1633	2010	2078
975	1	-2	-6	52	233	421	687	1581	2077	2021	2021
	2	2	-2	21	191	344	584	1148	1552	1864	1952
-1185	1	-4	-10	2	163	459	1137	1441	1763	2295	
	2	0	2	13	88	333	1007	1338	1688	1983	2042
1185	1	-4	-6	11	306	664	997	1261	1656	2544	3770
	2	0	0	11	262	679	1047	1338	1698	2057	2249
-1395	1	-6	-11	-13	-2	31	241	352	480	662	878
	2	-10	-15	-15	-10	10	237	379	536	720	926
1395	1	-2	-8	-15	-2	59	163	289	417	557	681
	2	-2	-8	-11	-4	2	46	178	346	530	718

Table IVb: T22. Strain in stirrups

x \ P		0.2	1.2	2.4	3.6	4.8	6.0	7.2	8.4	9.6	10.8	12.0	13.2
-538	1	0	-6	-8	21	72	154	238	314	408	1983		
	2	0	-4	-13	57	196	337	467	583	686	781	874	1006
538	1	0	-4	10	32	46	59	82	107	139	185	240	299
	2	0	-2	-17	2	65	149	227	295	371	446	518	581
-713	1	0	2	38	110	166	246	337	438	564	695	802	983
	2	0	-2	-10	-6	154	339	568	779	1055	1634	5263	
713	1	-2	-4	-8	19	46	97	232	478	648	764	926	1198
	2	0	0	11	74	141	244	451	716	1640	2579	3465	4288
-888	1	0	-2	2	51	118	196	293	389	524	630	1118	1922
	2	0	6	6	13	158	432	657	916	1198	1484	2305	
888	1	-2	-2	2	55	143	272	444	672	1027	1575	2842	4636
	2	-2	0	-10	0	187	341	526	792	1320	1960	2507	4690
-1063	1	0	-4	-11	36	234	467	730	1518	3310			
	2												
1063	1	0	-2	-6	10	61	158	444	653	733	1072	2672	
	2	-2	-2	0	30	202	570	964	1615	2181	2682	3234	3842
-1238	1	0	-4	-4	-2	29	278	598	836	1194	1834	3423	
	2	0	6	6	6	181	379	1103	1314	1697	2099	2674	
1238	1	-2	-2	-4	32	76	335	739	1994	2248	4189	5312	
	2	0	0	2	23	30	128		549		808	931	1488
-1413	1	-4	-6	-13	-17	-17	19	59	107	175	272	432	1078
	2	-4	-6	-8	-8	-10	-4	-2	10	32	82	225	659
1413	1	-2	-10	-19	-27	-21	34	131	387	575	810	1038	1270
	2	-2	-8	-13	-23	-21	-21	-25	-4	17	55	114	200

Table IVc: T23. Strain in stirrups

x \ P		0.2	1.2	2.4	3.6	4.8	6.0	7.2	8.4	9.6	10.8	12.0	13.2	14.2
-525	1	-2	-12	-2	8	42	98	171	254	408	525	633	746	792
	2	0	-8	-12	31	142	254	367	481	679	810	925	1044	1098
525	1	2	-8	-23	-12	17	54	100	146	208	262	312	367	442
	2	-4	-12	-25	8	73	163	254	335	435	519	587	667	773
-675	1	0	-2	10	31	83	127	225	348	748	958	1212	1717	2196
	2	0	-6	-4	40	169	213	275	354	531	733	1171	2750	5396
675	1	0	2	2	29	115	187	377	552	760	1088	1527	3127	4685
	2	4	2	29	117	223	288	410	594	815	1223	2604	3556	4304
-825	1													
	2													
825	1	2	-4	-6	-2	106	350	558	813	1163	1875	5290		
	2	0	-2	10	96	512	779	977	1188	1523				
-975	1	2	-4	-2	19	165	385	812	1256	1648	3088	5392		
	2	2	-2	4	33	152	327	715	1075	1338	2138	3658		
975	1	2	-2	-6	23	167	344	456	667	1033	2215	3379	5198	
	2	0	-2	-2	8	131	342	406	592	927	1688	2340	3806	
-1125	1	2	-2	2	19	152	525	885	1242	1998	2681	4208		
	2	2	0	2	27	137	502	821	1112	1587	2058	3629		
1125	1	2	-2	-2	8	77	306	548	844	1069	1569	2612	5248	
	2	2	-2	-2	4	13	806	1281	1921	3200	4721			
-1275	1	0	-6	-12	-15	38	429	921	1333	2225	3413	4710		
	2	2	-4	-10	-13	-4	185	565	887	1363	1596	1819	2317	
1275	1	6	-2	-4	13	31	546	946	1387	2075	4052			
	2	0	-4	-4	2	2	181	394	679	1012	1158	1250	1415	2179
-1425	1	4	-12	-23	-46	-58	-54	-6	69	196	323	502	792	1013
	2	2	-10	-17	-37	-44	-44	-48	-40	31	119	256	481	640
1425	1	0	-4	-6	-15	-13	13	81	185	319	498	700	1040	1188
	2	2	-2	-2	-10	-6	8	12	35	100	212	356	617	769

P in Mp, excl. of weight of beam 0.15 Mp/m
x in mm. Strain in 10^{-6} mm/mm

Table Va: T21. Deflection of tension and compression flange

	x \ P	1.3	2.6	3.9	5.2	6.5	7.8	9.1	10.4	11.7
tension	1395	0.0	0.2	0.4	0.7	1.0	1.3	1.6	1.9	2.3
	1185	0.0	0.4	0.8	1.4	2.0	2.7	3.4	4.3	5.2
	975	0.0	0.5	1.2	2.1	3.0	3.9	5.0	6.3	7.8
	765	0.0	0.7	1.6	2.7	3.8	5.1	6.5	8.0	9.8
	555	0.0	0.8	1.8	3.1	4.4	5.9	7.5	9.3	11.3
	0	0.0	1.0	2.2	3.7	5.2	6.8	8.5	10.6	12.9
	-555	0.0	0.8	1.9	3.2	4.5	6.0	7.5	9.4	11.4
	-765	0.0	0.7	1.6	2.7	3.8	5.1	6.4	8.1	10.0
	-975	0.0	0.5	1.2	2.0	2.9	3.9	5.0	6.3	7.8
	-1185	0.0	0.4	0.8	1.3	1.9	2.6	3.3	4.3	5.2
	-1395	0.0	0.2	0.4	0.6	0.9	1.1	1.4	2.0	2.3
compression	1395	0.0	0.1	0.4	0.7	1.0	1.1	1.4	1.7	2.1
	1185	0.0	0.3	0.8	1.4	1.8	2.3	2.9	3.5	4.1
	975	0.0	0.5	1.2	2.1	2.9	3.7	4.5	5.4	6.5
	765	0.0		1.5	2.6	3.7	4.7	6.0	7.3	8.9
	555	0.0	0.8	2.0	3.3	4.6	5.9	7.5	9.2	11.0
	0	0.0	0.9	2.2	3.7	5.1	6.8	8.6	10.5	12.6
	-555	0.0	0.8	1.9	3.2	4.5	5.8	7.6	9.1	10.9
	-765	0.0	0.8	1.6	2.7	3.7	4.8	6.1	7.4	8.7
	-975	0.0	0.5	1.0	2.0	2.7	3.3	4.4	5.3	6.2
	-1185	0.0	0.4	0.8	1.3	1.8	2.1	2.9	3.4	4.0
	-1395	0.0	0.2	0.4	0.6	0.9	1.2	1.4	1.7	2.0

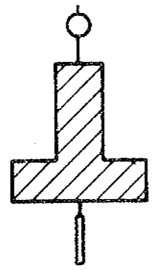

P in Mp
x in mm
Deflec. in mm

Table Vb: T22. Deflection of tension and compression flange

	x \ P	0.2	1.2	2.4	3.6	4.8	6.0	7.2	8.4	9.6	10.8	12.0
tension	1413	0.0	0.1	0.2	0.4	0.6	0.8	0.9	1.1	1.3	1.6	1.8
	1238	0.0	0.2	0.5	0.8	1.2	1.6	2.0	2.5	3.0	3.6	4.3
	1063	0.0	0.3	0.7	1.2	1.8	2.4	3.1	3.8	4.5	5.4	6.3
	888	0.0	0.3	0.9	1.6	2.3	3.2	4.0	4.9	5.9	7.1	8.5
	712	0.0	0.4	1.1	1.9	2.8	3.8	4.8	5.9	7.0	8.4	10.0
	538	0.0	0.5	1.3	2.2	3.2	4.3	5.4	6.7	7.9	9.4	11.2
	0	0.0	0.5	1.5	2.5	3.6	4.9	6.1	7.4	8.8	10.3	12.3
	-537	0.0	0.5	1.3	2.2	3.2	4.2	5.3	6.4	7.6	9.1	10.9
	-712	0.0	0.4	1.1	1.9	2.8	3.7	4.6	5.6	6.6	7.9	9.6
	-887	0.0	0.3	0.9	1.5	2.3	3.1	3.8	4.6	5.5	6.6	7.9
	-1062	0.0	0.3	0.7	1.2	1.7	2.3	2.8	3.4	4.1	5.0	6.1
	-1237	0.0	0.2	0.5	0.8	1.1	1.5	1.8	2.2	2.6	3.2	3.8
	-1412	0.0	0.1	0.3	0.4							
compression	1413	0.0	0.1	0.3	0.5	0.6	0.8	1.0	1.1	1.2	1.6	1.9
	1238	0.0	0.1	0.3	0.8	1.2	1.4	1.9	2.1	2.6	3.0	3.5
	1063	0.0	0.2	0.6	1.2	1.6	2.2	2.8	3.4	3.9	4.7	5.4
	888	0.0	0.2	0.7	1.5	2.2	2.9	3.8	4.6	5.4	6.4	7.5
	712	0.0	0.3	1.0	1.9	2.8	3.6	4.7	5.6	6.7	8.0	9.4
	538	0.0	0.4	1.1	2.0	3.0	4.0	5.1	6.3	7.6	9.0	10.6
	0	0.0	0.7	1.4	2.7	3.8	5.1	6.3	7.6	9.1	10.8	12.8
	-537	0.0	0.5	1.1	2.2	3.2	4.1	5.4	6.3	7.6	9.0	10.7
	-712	0.0	0.4	1.0	1.9	2.8	3.6	4.7	5.8	6.7	8.1	9.4
	-887	0.0	0.3	0.8	1.5	2.3	3.0	3.8	4.6	5.5	6.5	7.5
	-1062	0.0	0.2	0.5	1.1	1.7	2.2	2.8	3.4	4.0	4.7	5.4
	-1237	0.0	0.2	0.4	0.8	1.2	1.6	2.5	2.3	2.7	3.3	3.5
	-1412	0.0	0.0	0.2	0.5	0.7	0.7	1.0	1.2	1.4	1.6	1.8

Table Vc: T23. Deflection of tension and compression flange

	x \ P	0.2	1.2	2.4	3.6	4.8	6.0	7.2	8.4	9.6	10.8	12.0	13.2
tension	1425	0.0	-0.1	0.0	0.2	0.4	0.6	0.7	0.8	1.0	1.2	1.5	1.7
	1275	0.0	0.1	0.3	0.6	0.9	1.3	1.7	2.1	2.6	3.1	3.7	4.6
	1125	0.0	0.2	0.5	1.0	1.4	2.0	2.6	3.2	3.8	4.6	5.5	6.9
	975	0.0	0.2	0.6	1.2	1.9	2.6	3.4	4.1	5.0	6.1	7.3	9.1
	825	0.0	0.2	0.8	1.5	2.3	3.2	4.1	5.0	6.1	7.4	8.8	11.0
	675	0.0	0.3	1.0	1.8	2.7	3.8	4.8	5.9	7.1	8.5	10.1	12.5
	525	0.0	0.4	1.2	2.1	3.1	4.3	5.4	6.5	7.8	9.4	11.0	13.5
	0	0.0	0.3	1.2	2.3	3.4	4.7	6.0	7.2	8.7	10.3	12.1	14.8
	-525	0.0	0.3	1.1	2.0	3.0	4.1	5.3	6.4	7.7	9.2	10.8	13.3
	-675	0.0	0.4	1.1	1.9	2.8	3.8	4.8	5.8	7.0	8.3	9.7	12.1
	-825	0.0	0.4	0.9	1.6	2.4	3.3	4.2	5.1	6.1	7.2	8.6	10.8
	-975	0.0	0.3	0.7	1.3	1.9	2.6	3.3	4.1	4.9	5.9	7.0	8.8
	-1125	0.0	0.3	0.6	1.0	1.5	2.0	2.5	3.1	3.7	4.3	5.1	6.2
	-1275	0.0	0.2	0.4	0.7	0.9	1.3	1.6	2.0	2.4	2.8	3.3	3.9
	-1425	0.0	0.3	0.4	0.4	0.5	0.6	0.7	0.9	1.0	1.0	1.1	1.3
compression	1425	0.0	0.1	0.3	0.4	0.5	0.7	0.9	1.1	1.2	1.4	1.5	1.7
	1275	0.0	0.2	0.4	0.7	1.0	1.3	1.6	1.9	2.4	2.7	3.0	3.3
	1125	0.0	0.1	0.6	0.9	1.3	1.9	2.4	2.8	3.4	3.9	4.4	5.1
	975	0.0	0.3	0.7	1.2	1.9	2.6	3.3	4.0	4.8	5.5	6.2	7.1
	825	0.0	0.3	0.8	1.5	2.3	3.2	4.0	4.9	5.9	6.9	8.6	9.4
	675	0.0	0.4	1.2	1.9	2.8	3.9	4.8	5.9	7.0	8.3	9.6	11.6
	525	0.0	0.4	1.1	1.9	2.9	3.9	5.1	6.0	7.4	8.7	10.1	12.3
	0	0.0	0.5	1.4	2.3	3.6	4.8	6.1	7.4	8.8	10.6	12.3	15.1
	-525	0.0	0.4	1.1	1.9	2.9	4.0	5.0	6.2	7.4	8.7	10.3	12.4
	-675	0.0	0.4	1.1	1.8	2.8	3.8	4.8	5.8	7.0	8.2	9.5	11.4
	-825	0.0	0.4	1.0	1.5	2.5	3.3	4.1	4.9	5.9	6.9	7.9	9.2
	-975	0.0	0.3	0.9	1.3	2.0	2.7	3.3	4.1	4.8	5.5	6.2	7.1
	-1125	0.0	0.3	0.6	1.0	1.5	2.0	2.5	3.0	3.5	4.0	4.5	5.1
	-1275	0.0	0.3	0.5	0.7	1.0	1.4	1.7	2.1	2.4	2.7	3.0	3.3
	-1425	0.0	0.1	0.2	0.3	0.6	0.6	0.9	1.0	1.2	1.3	1.5	1.6

Table VI, Series I: Strain along longotudinal reinforcement and compression flange,

T21	P: exclusive of weight of beam 0.15 Mp/m						
No.	P (Mp)	-2 o/oo	-1 o/oo	t o/oo	+1 o/oo	+2 o/oo	c o/oo
1	0.2	0.13	0.10	0.04	-0.04	-0.05	0.02
2	1.2	0.07	0.17	0.08	0.07	-0.12	-0.02
3	2.4	0.11	0.33	0.33	0.23	-0.15	-0.07
4	3.6	0.13	0.53	0.49	0.43	0.03	-0.12
5	4.8	0.28	0.79	0.66	0.59	0.03	-0.17
6	6.0	0.28	0.95	0.89	0.83	0.22	-0.19
7	7.2	0.42	1.14	1.12	0.93	0.29	-0.26
8	8.4	0.51	1.28	1.32	1.06	0.36	-0.36
9	9.6	0.72	1.55	1.46	1.31	0.59	-0.46
10	10.8	0.80	1.75	1.65	1.52	0.68	-0.52
11	12.0	0.98	1.98	1.84	1.78	0.89	-0.68
T22	P: exclusive of weight of beam 0.15 Mp/m						
No.	P (Mp)	-2 o/oo	-1 o/oo	t o/oo	+1 o/oo	+2 o/oo	c o/oo
1	1.3	0.03	0.14	0.14	0.13	0.01	-0.05
2	2.6	0.12	0.30	0.28	0.30	0.04	-0.09
3	3.9	0.14	0.53	0.55	0.53	0.10	-0.15
4	5.2	0.29	0.74	0.76	0.76	0.23	-0.20
5	6.5	0.41	0.99	0.96	0.93	0.36	-0.27
6	7.8	0.55	1.23	1.18	1.18	0.56	-0.33
7	9.1	0.72	1.44	1.40	1.40	0.69	-0.40
8	10.4	0.85	1.72	1.62	1.59	0.85	-0.47
9	11.7	1.05	1.87	1.85	1.79	1.04	-0.55
T23	P: exclusive of weight of beam 0.15 Mp/m + 0.2 Mp						
No.	P (Mp)	-2 o/oo	-1 o/oo	t o/oo	+1 o/oo	+2 o/oo	c o/oo
2	1.2	0.00	0.05	0.09	0.08	0.08	-0.08
3	2.4	-0.02	0.21	0.26	0.22	0.10	-0.13
4	3.6	0.03	0.33	0.46	0.44	0.12	-0.17
5	4.8	0.09	0.58	0.68	0.64	0.21	-0.21
6	6.0	0.21	0.68	0.90	0.80	0.31	-0.24
7	7.2	0.31	0.93	1.06	0.96	0.42	-0.37
8	8.4	0.41	1.07	1.23	1.19	0.63	-0.35
9	9.6	0.56	1.29	1.38	1.42	0.80	-0.43
10	10.8	0.74	1.51	1.62	1.62	0.94	-0.53
11	12.0	0.94	1.55	1.79	1.77	1.14	-0.55
12	13.2	1.17	1.84	2.04	2.08	1.29	-0.59

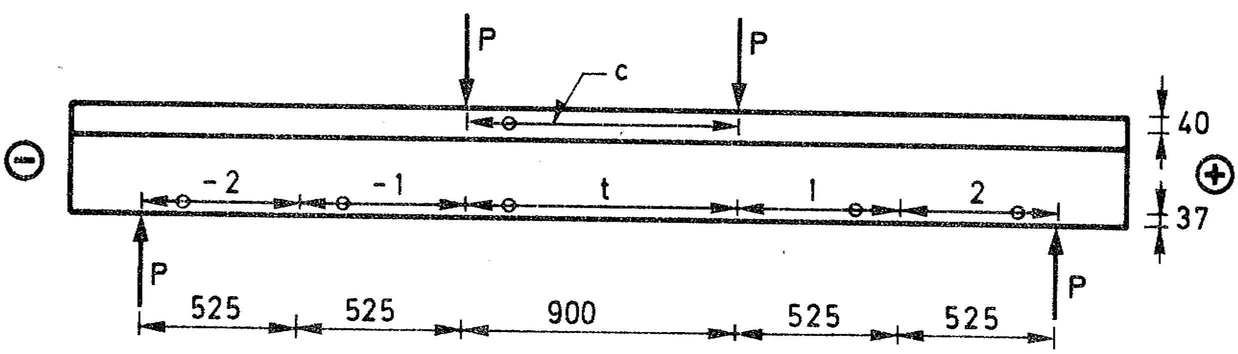

Dimensions in mm

Table VII, Series II: Strain along longitudinal reinforcement and compression flange, dial gauges. Numbers of cracks.

T1a

No.	P Mp	c o/oo	t o/oo
d		44	57
1	1.5	-0.05	0.12
2	3.0	-0.12	0.36
3	4.5	-0.18	0.59
4	6.0	-0.25	0.80
5	7.5	-0.32	1.03
6	9.0	-0.40	1.26
7	10.5	-0.50	1.49
8	12.0	-0.60	1.73
9	13.5	-1.06	7.18

T2a

No.	P Mp	c o/oo	t o/oo
d		43	57
1	1.3	-0.05	0.10
2	2.6	-0.10	0.31
3	3.9	-0.15	0.53
4	5.2	-0.21	0.72
5	6.5	-0.26	0.93
6	7.8	-0.32	1.12
7	9.1	-0.39	1.33
8	10.4	-0.47	1.54
9	11.7	-0.56	1.76
10	13.0	-0.66	2.10
11	13.6	-0.77	3.18
11	13.6	-0.85	4.41
11	13.9	-1.07	7.30

T3a

No.	P Mp	c o/oo	t o/oo
d		34	57
1	1.3	-0.05	0.11
2	2.6	-0.12	0.33
3	3.9	-0.17	0.51
4	5.2	-0.23	0.71
5	6.5	-0.30	0.91
6	7.8	-0.35	1.11
7	9.1	-0.42	1.31
8	10.4	-0.49	1.51
9	11.7	-0.60	1.73
10	13.0	-0.60	1.93

T4a

No.	P Mp	c o/oo	t o/oo
d		43	57
1	1.3	-0.05	0.12
2	2.6	-0.12	0.32
3	3.9	-0.17	0.51
4	5.2	-0.23	0.71
5	6.5	-0.27	0.90
6	7.8	-0.32	1.10
7	9.1	-0.40	1.29
8	10.4	-0.48	1.51
9	11.7	-0.55	1.71
10	13.0	-0.63	1.95
11	13.5	-0.64	2.06

T1b

No.	P Mp	c o/oo	t o/oo
d		32	57
1	1.2	-0.06	0.12
2	2.4	-0.10	0.27
3	3.6	-0.16	0.46
4	4.8	-0.21	0.65
5	6.0	-0.26	0.82
6	7.2	-0.32	1.00
7	8.4	-0.38	1.17
8	9.6	-0.45	1.37
9	10.8	-0.53	1.55
10	12.0	-0.64	1.72

T2b

No.	P Mp	c o/oo	t o/oo
d		36	57
1	1.2	-0.04	0.08
2	2.4	-0.12	0.26
3	3.6	-0.16	0.46
4	4.8	-0.23	0.65
5	6.0	-0.28	0.82
6	7.2	-0.35	1.01
7	8.4	-0.42	1.18
8	9.6	-0.50	1.36
9	10.8	-0.58	1.56
10	12.0	-0.68	1.75
11	13.2	-0.91	2.00

T3b

No.	P Mp	c o/oo	t o/oo
d		35	57
1	1.0	-0.03	0.07
2	2.0	-0.08	0.21
3	3.0	-0.12	0.37
4	4.0	-0.17	0.52
5	5.0	-0.21	0.67
6	6.0	-0.25	0.82
7	7.0	-0.30	0.96
8	8.0	-0.34	1.11
9	9.0	-0.40	1.27
10	10.0	-0.44	1.42
11	11.0	-0.51	1.57
12	11.8	-0.56	1.70

T4b

No.	P Mp	c o/oo	t o/oo
d		40	57
1	1.0	-0.04	0.07
2	2.0	-0.08	0.18
3	3.0	-0.15	0.36
4	4.0	-0.20	0.51
5	5.0	-0.25	0.68
6	6.0	-0.31	0.84
7	7.0	-0.35	0.99
8	8.0	-0.41	1.14
9	9.0	-0.47	1.29
10	10.0	-0.53	1.43
11	10.9	-0.58	1.58

T5

No.	P Mp	c o/oo	t o/oo
d		35	57
1	1.2	-0.04	0.09
2	2.25	-0.09	0.26
3	3.3	-0.14	0.45
4	4.4	-0.18	0.62
5	5.5	-0.24	0.79
6	6.6	-0.29	0.95
7	7.7	-0.36	1.12
8	8.8	-0.42	1.30
9	9.9	-0.47	1.49
10	10.4	-0.51	1.55

P: exclusive of weight of beam 0.15 Mp/m

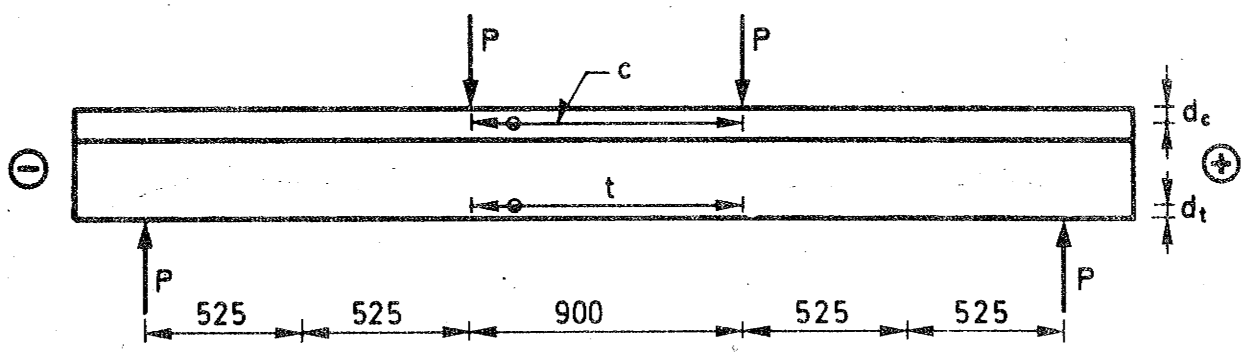

Dimensions in mm

Table VIII, Series I: Maximum crack widths

P (Mp)	Flexure (mm)	Shear + (mm)	Shear - (mm)
T21			
10.4	0.1	0.6	0.7
11.7	0.1	0.8	1.0
T22			
7.2	<0.05	0.05	0.15
9.6	0.2	0.25	0.3
10.8	0.1	0.3	0.35
12.0	0.25	0.8	0.9
T23			
7.2	<0.05	0.2	0.15
8.4	<0.05	0.25	0.15
9.6	0.1	0.3	0.3
10.8	0.1	0.55	0.55
12.0	0.1	0.9	1.1
13.2	0.15	1.5	1.5

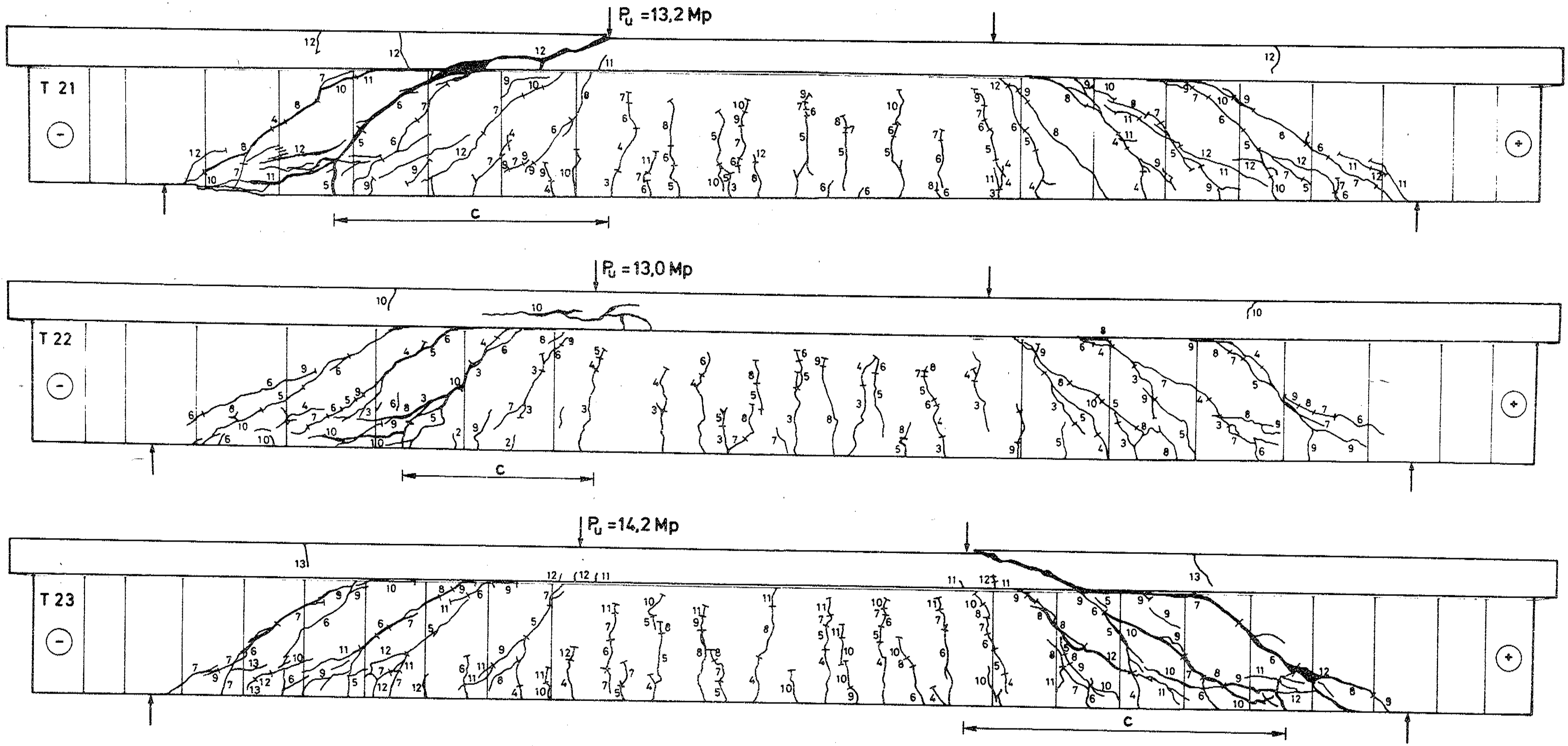

Fig.2.10a: Crack pattern after failure, beam T21, T22, T23

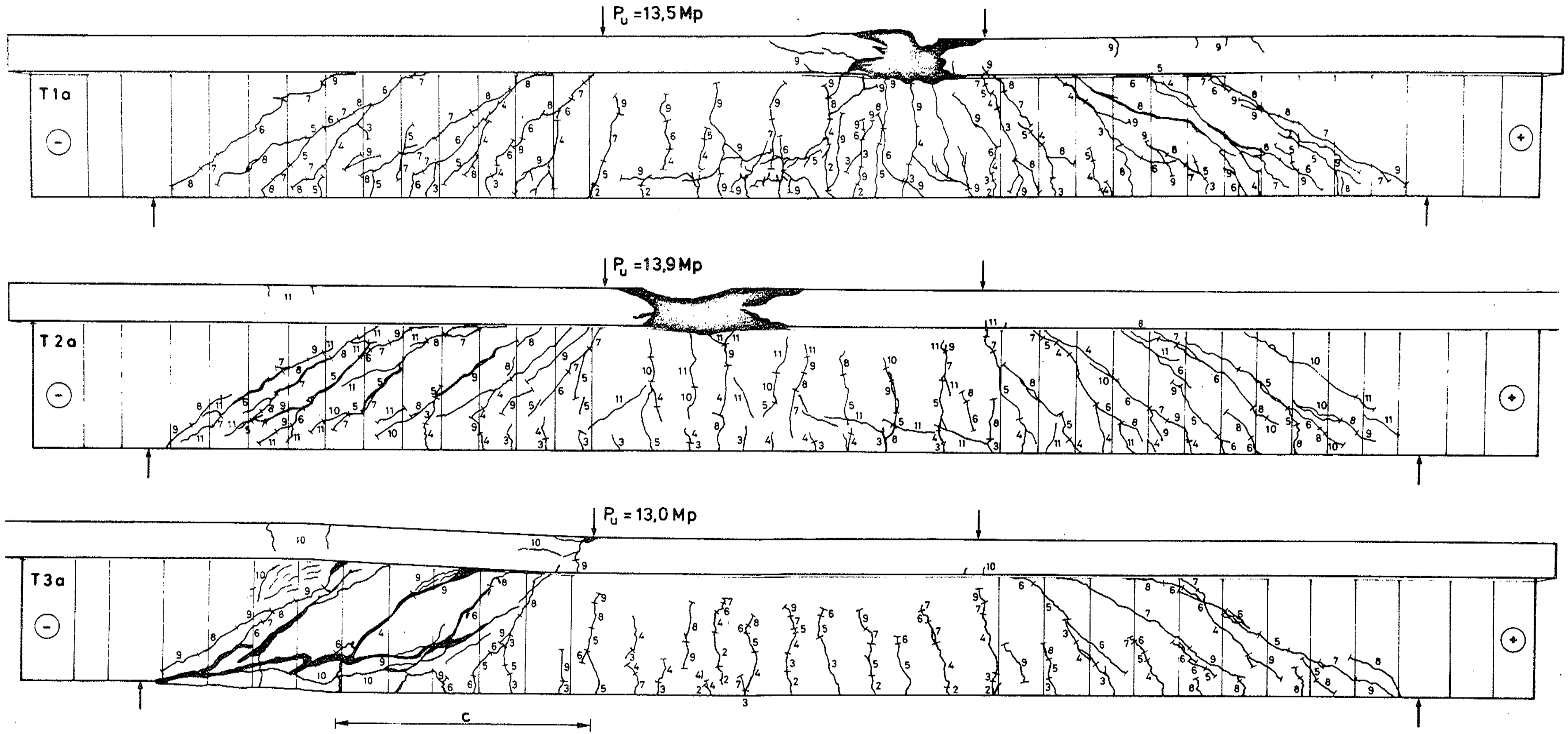

Fig.2.10b: Crack pattern after failure, beam T1a, T2a, T3a

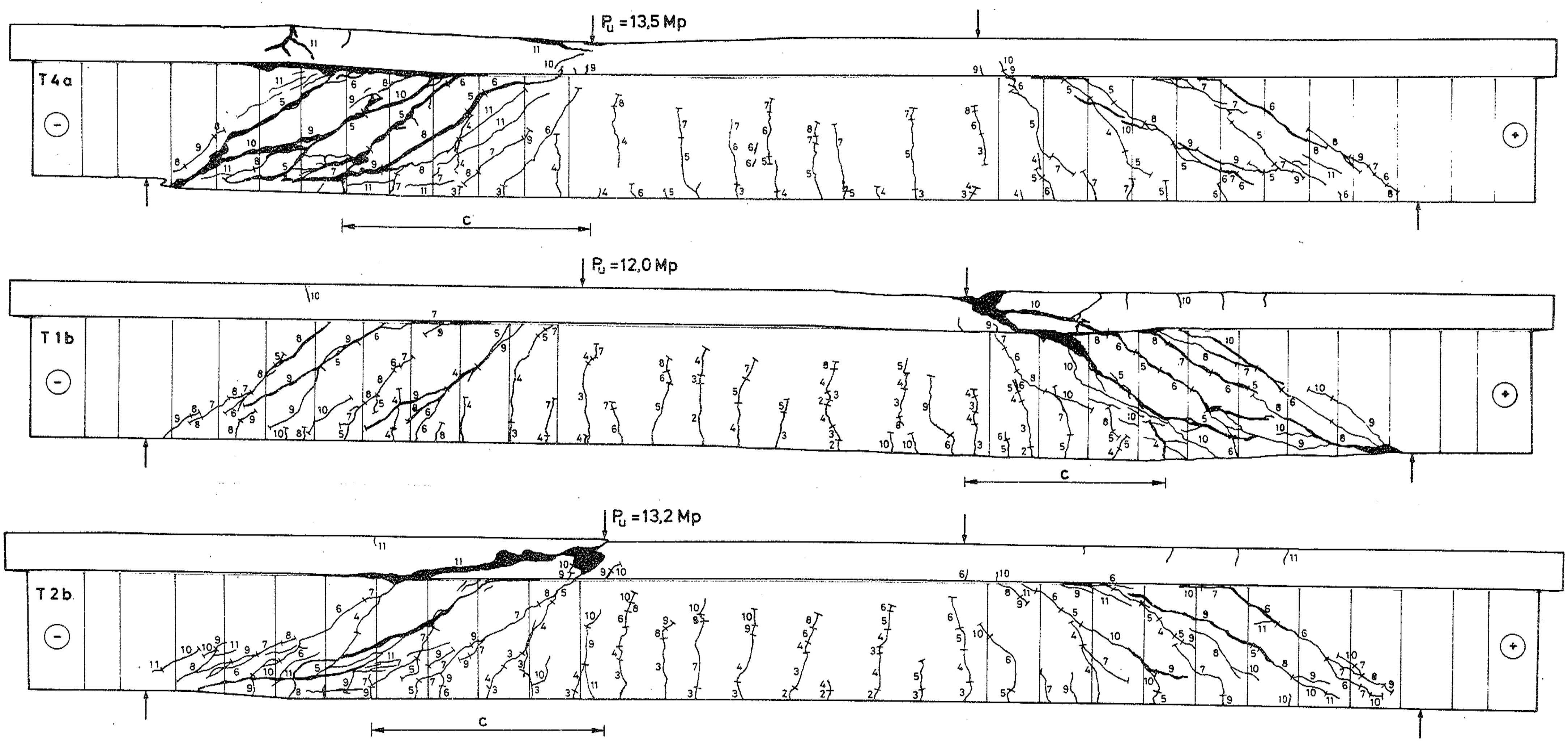

Fig.2.10c: Crack pattern after failure, beam T4a, 1b, 2b

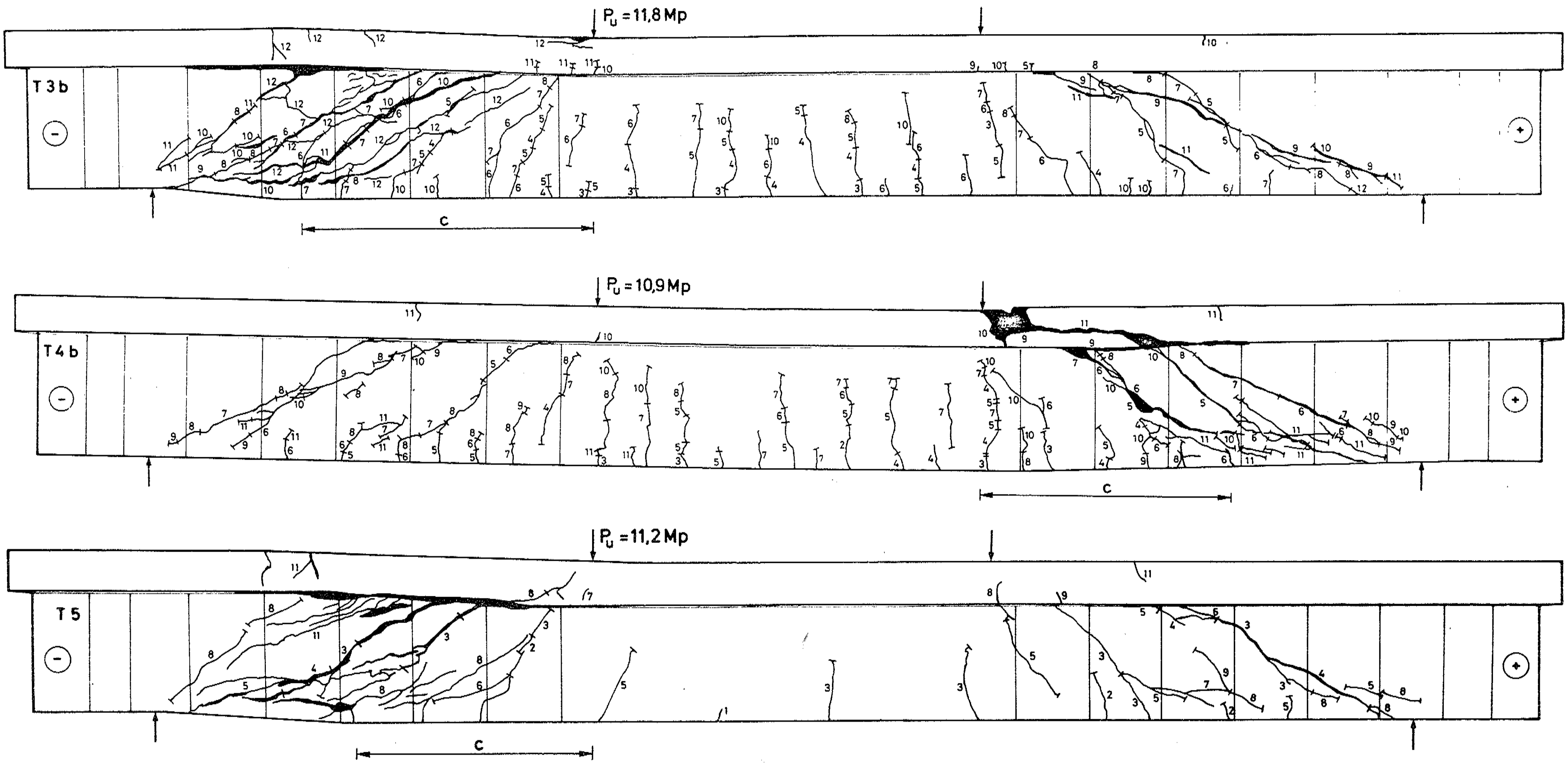

Fig.2.10d: Crack pattern after failure, beam T3b, T4c, T5

AFDELINGEN FOR BÆRENDE KONSTRUKTIONER
DANMARKS TEKNISKE HØJSKOLE

Structural Research Laboratory
Technical University of Denmark, DK-2800 Lyngby

RAPPORTER (Reports)
(1971 -

R 20.	Sørensen, Hans Christian: Forskydningsforsøg med 12 jernbetonbjælker med T-tværsnit. 1971.	
R 21.	Møllmann, H.: Analysis of Hanging Roofs Using the Displacement Method. 1971.	Out of print
R 22.	Haurbæk, Poul E.: Dæmpede svingninger i spændbetonbjælker. Svingningsforsøg med simpelt understøttede bjælker.	Publication pending
R 23.	Bræstrup, M.W.: Yield-line Theory and Limit Analysis of Plates and Slabs. 1971.	
R 24.	Dyrbye, Claës: Pendulum Vibration. 1971.	Out of print
R 25.	Møllmann, H.: Analytical Solution for a Cable Net over a Rectangular Plan. 1971.	
R 26.	Nielsen, J.: Silotryk. 1972.	Out of print
R 27.	Askegaard, V., M. Bergholdt and J. Nielsen: Problems in connection with pressure cell measurements in silos. 1972.	
R 28.	Ramirez, H. Daniel: Buckling of plates by the Ritz method using piecewise-defined functions. 1972.	
R 29.	Thomsen, Kjeld & Henning Agerskov: Behaviour of butt plate joints in rolled beams assembled with prestressed high tensile bolts. 1972.	
R 30.	Julius Solnes and Ragnar Sigbjörnsson: Structural response to stochastic wind loading. 1972.	
R 31.	H. J. Larsen og H. Riberholt: Forsøg med uklassificeret konstruktionstræ. 1972.	
R 32.	Vagn Askegaard: Programme and methods of teaching of experimental mechanics. 1972.	Out of print
R 33.	Julius Solnes and Ole Holst: Weight optimization of framed structures under earthquake loads. 1972.	
R 34.	Rostam, Steen and Esben Byskov: Cracks in Concrete Structures. A Fracture Mechanics Approach. 1973.	
R 35.	Sørensen, Hans Chr.: Efficiency of Bent-up Bars as Shear Reinforcement. 1973.	
R 36.	Krenk, Steen: Singulær integralformulering af nogle plane friktionsfri kontaktproblemer. 1973.	
R 37.	Philipsen, Claus: An investigation of the stability of columns with thin-walled open cross-section. 1973.	

R 38. Theilgaard, Esko: Integralligningsmetoder anvendt på problemer inden for bygningsstatikken. 1973.

R 39. Henrichsen, Lars: Linearly viscoelastic finite elements. 1973.

R 40. Bryndum, Mads: Litteraturstudium vedrørende let konstruktionsbeton. 1973.

R 41. Holst, Ole: Beregning af plane rammekonstruktioner med geometrisk ikkelinearitet. 1973.

R 42. Krenchel, Herbert: Rupture criteria for FRC-materials. 1973.

R 43. Borchersen, Egil: Moiré pattern deformation theory and optical filtering techniques. 1974.

R 44. Brøndum-Nielsen, Troels: Optimum design of reinforced concrete shells and slabs. 1974.

R 45. Pedersen, Flemming Bligaard: Dynamic properties of anti-vibration mountings. 1974.

R 46. Philipsen, Claus: Interferensholografisk bestemmelse af legemers form og flytningsfelt. 1974.

R 47. Larsen, H.J. og H. Riberholt: Tværbæreevne af søm og dykkere i spån- og træfiberplader. 1974.

R 48. Poulsen, P.E.: The photo-elastic effect in three--dimensional states of stress. 1974.

R 49. Nielsen, J.: Modellove for kornede medier med særligt henblik på silomodeller. 1974.

R 50. Krenk, Steen: The problem of an inclined crack in an elastic strip. 1974.

R 51. Brøndum-Nielsen, Troels: Effect of prestress on the damping of concrete. Effect of grouting on the fatigue strength of post-tensioned concrete beams. 1974.

R 52. Egerup, Arne Ryden, H. J. Larsen, H. Riberholt and Erik Sørensen: Papers presented at IUFRO-V, International Union of Forestry Research Organisation, Division V, Congress 1973. 1974.

R 53. Holst, Ole: Automatic design of plane frames. 1974.

R 54. Nielsen, Søren: Svingninger i mastebarduner I. 1974.

R 55. Agerskov, Henning: Behaviour of connections using prestressed high strength bolts loaded in tension. 1974.

R 56. Møllmann, H.: Analysis of prestressed cable systems supported by elastic boundary structures. 1974.

R 57. Nielsen, J. and V. Askegaard: Scale errors in model tests on granular media with special reference to silo models. 1974.

R 58. Svensson, Sven Eilif: Stability properties and mode interaction of continuous, conservative systems. 1974.